Valna opterećenja oštećenog broda

Mikulić, Antonio

Master's thesis / Diplomski rad

2016

Permanent link / Trajna poveznica: https://urn.nsk.hr/urn:nbn:hr:235:728434

Download date / Datum preuzimanja: **2024-04-16**

Repository / Repozitorij:

Repository of Faculty of Mechanical Engineering and Naval Architecture University of Zagreb

UNIVERSITY OF ZAGREB
FACULTY OF MECHANICAL ENGINEERING AND NAVAL
ARCHITECTURE

MASTER'S THESIS

Antonio Mikulić

Zagreb, 2016.

UNIVERSITY OF ZAGREB
FACULTY OF MECHANICAL ENGINEERING AND NAVAL
ARCHITECTURE

MASTER´S THESIS

Supervisors: Student:

JoškoParunov, Professor (University of Zagreb)   Antonio Mikulić

Zagreb, 2016.

SVEUČILIŠTE U ZAGREBU
FAKULTET STROJARSTVA I BRODOGRADNJE
Središnje povjerenstvo za završne i diplomske ispite
Povjerenstvo za završne i diplomske ispite studija brodogradnje

DIPLOMSKI ZADATAK

Student: **Antonio Mikulić**   Mat. br.: 0035182006

Naslov rada na
hrvatskom jeziku: **VALNA OPTEREĆENJA OŠTEĆENOG BRODA**

Naslov rada na
engleskom jeziku: **ASSESSMENT OF GLOBAL VERTICAL LOADS IN DAMAGED SHIP**

Opis zadatka:

The objective of the thesis is to study the effect of flooded compartments on a ship regarding the global vertical loads in the presence of waves. 3D panel hydrodynamic code WAMIT will be used in the analysis. WAMIT provides hydrodynamic coefficients and excitation as well as transfer functions of ship motion.

As a first step, it is necessary to develop MATLAB tool for calculating transfer functions of wave-induced global loads along the vessel as well as for graphical presentation of results.

After modelling the side shell of double hull oil tanker and its compartments, the student must also develop a MATLAB tool able to call WAMIT to simulate the ship behaviour for different flooded conditions. Transfer functions of ship motion and global wave induced loads will then be calculated and plotted using tool developed in the first step.

The obtained results are to be compared with others already published, in particular in refs. [1] and [2]. Analysis of results will provide relevant conclusions and indicate further work.

References:

[1]   Parunov, J., Ćorak, M., Gledić, I. Comparison of two practical methods for seakeeping assessment of damaged ships. Analysis and Design of Marine Structures V. Guedes Soares, C., Shenoi, R. A. (ur.). London : Taylor & Francis Group, 2015., 37-44.

[2]   Parunov, J., Ćorak, M. Design charts for quick estimation of wave loads on damaged oil tanker in the Adriatic Sea. Towards Green Marine Technology and Transport. Guedes Soares C., Dejhalla R., Pavletic D. (ur.). London, UK : Taylor & Francis Group, 2015., 389-395.

Zadatak zadan:

5. svibnja 2016.

Zadatak zadao:

Prof. dr. sc. Joško Parunov

Rok predaje rada:

7. srpnja 2016.

Predviđeni datumi obrane:

13., 14. i 15. srpnja 2016.

Predsjednica Povjerenstva:

Prof. dr. sc. Nastia Degiuli

I declare that I have done this work independently using the knowledge acquired during studies and cited references.

Antonio Mikulić

CONTENTS

LIST OF FGURES

LIST OF TABLES

LIST OF SIMBOLS

∇	m^3	displacement volume
$[A_{ij}]$		added mass matrix
$[B_{ij}]$		matrix of damping coefficients
$[C_{ij}]$		matrix of hydrostatic and restoring coefficients
$[M_{ij}]$		generalised mass matrix
$\{F_i\}$		vector of exciting forces and moments
$A_{p,i}$	m^2	surface of panel
$a_z(x)$	m/s^2	local absolute acceleration
B	m	ship's breadth
C	-	constant
D	m	ship's depth
DWT	t	ship's deadweight
$f(x)$	kN/m	distribution of fluid forces over the wetted surface of the hull
$f_{hp}(x)dx$	kN	hydrodynamic pressure force
$f_r(x)dx$	kN	restoring force
g	m/s^2	acceleration of gravity
h	m	water depth
I_{ij}	t m^2	moments of inertia
k	rad/m	wave number
LCG/x_g	m	longitudinal center of gravity
L_{PP}	m	length between perpendiculars
m	t	body mass
$m(x)$	t	local mass of the ship
$M(x_1)$	kNm	shear force at a section whose x-coordinate is x_1
$\boldsymbol{n}$	-	normal vector
$n_{3,i}$		z-component of panel surface normal vector
p	Pa	pressure
p_i	Pa	the pressure acting on the surface of the panel
p_o	Pa	atmospheric pressure
$q(x)$	kN/m	longitudinally distributed net vertical force per unit length
RAO_3	m/m	response amplitude operator of heave motion
RAO_5	deg/m	response amplitude operator of pitch motion
r_{ij}	m	radii of gyration
S_b	m^2	wetted surface
t	s	time
T	m	ship's drought
TCG/y_g	m	transversal center of gravity

T_s	s^{-1}	wave period
$\boldsymbol{u}$	-	body velocity vector
u	m/s	component of body velocity vector in direction of x-axes
$\boldsymbol{v}$	m/s	velocity vector
v	m/s	component of body velocity vector in direction of y-axes
$V(x_1)$	kN	shear force at a section whose x-coordinate is x_1
VCG/z_g	m	vertical center of gravity
w	m/s	component of body velocity vector in direction of z-axes
$\boldsymbol{x}$	-	point in space
x_b	m	longitudinal center of buoyancy
x_P	m	absolute harmonic motion in x direction
y_b	m	transversal center of buoyancy
y_P	m	absolute harmonic motion in y direction
z_b	m	vertical center of buoyancy
z_{gi}	m	distance between VCG and a steadily translating coordinate system
z_P	m	absolute harmonic motion in z direction
Φ	m^2/s	velocity potential
Φ_0	m^2/s	incident wave velocity potential
Φ_7	m^2/s	scattered wave velocity potential
Φ_D	m^2/s	diffraction wave velocity potential
Φ_j	m^2/s	unit-amplitude radiation potential
Φ_R	m^2/s	radiation wave velocity potential
β	deg	wave heading angle
η_1		surge motion
η_2		sway motion
η_3		heave motion
η_4		roll motion
η_5		pitch motion
η_6		yaw motion
λ	m	wavelength
ρ	t/m^3	water density
$\boldsymbol{\omega}$	-	vorticity vector
ω	rad/s	circular wave frequency
ζ	m	wave surface elevation function
ζ_a	m	wave amplitude
ζ_i	m	the complex amplitudes of the body oscillatory motion in its six rigid-body degrees of freedom

ABBREVATION

2D	two-dimensional
3D	three-dimensional
AFRAMAX	Size of tanker, deadweight under 120000 tons and breadth more than 32.31 m
AP	aft peak
CAD	computer-aided design
CFG	Configuration file
CSR-H	Harmonized Common Structural Rules
CT	cargo tanks
DC	damage case
DNV	Det Norske Veritas
EU	European Union
FP	fore peak
FRC	Force Control File
GDF	Geometric Data File
IACS	International Association of Classification Societies
IMO	International Maritime Organization
ISO	International Organization for Standardization
MC	Monte Carlo
POT	Potential Control File
PS	port side
RAO	response amplitude operator
SB	starboard side
SNAME	The Society of Naval Architects and Marine Engineers
UK	United Kingdom
US	United States
VWBM	vertical wave-induced bending moment
VWSF	vertical wave-induced shear force
WBT	water ballast tank

SAŽETAK

Diplomskim radom analizirana su globalna valna opterećenja u slučaju naplavljivanja oštećenog broda. Analiza pomorstvenosti provedena je uz pretpostavku trodimenzionalnog linearnog potencijalnog strujanja sa slobodnom površinom korištenjem numeričke metode rubnih elemenata, programirane u računalnom kodu WAMIT. Budući da rezultati analize u WAMIT-u ne sadrže globalna valna opterećenja, već samo hidrodinamičke tlakove na oplakanoj površini i prijenosne funkcije gibanja, u programskom sučelju MATLAB izrađen je u tu svrhu odgovarajući programski kod. Razvijeni kod na temelju prethodno navedenih izlaznih rezultata i definirane distribucije masa računa vertikalne valne smične sile i momente savijanja.

Proračun vertikalnih valnih opterećenja proveden je prema vrpčastoj metodi. Brod je po duljini diskretiziran na segmente pune širine i visine, a ograničene duljine (vrpce). Za svaku vrpcu računaju se hidrodinamičke, povratne i inercijske sile, a zatim se numeričkom integracijom (odabrana je trapezna metoda) računaju globalna valna opterećenja.

Uz računanje vertikalnih globalnih valnih opterećenja navedeni kod, na temelju definirane geometrije trupa i tankova, automatski generira ulazne datoteke potrebne za analizu u WAMIT-u te pokreće simulaciju.

Trodimenzionalni model i mreža trupa broda i njegovi odjeljci modelirani su u programu Rhinoceros. Mreža je u svrhu olakšanja numeričke integracije definirana u skladu sa dimenzijama pojedinih vrpci, tj. cjelokupna površina panela mora biti unutar jedne vrpce.

Provedene su simulacije za brod u neoštećenom stanju te 8 slučajeva uslijed naplavljivanja oštećenog broda. Naplavljena tekućina u tanku nalazi se u razini vodne linije, dok je oplata tanka zbog pojednostavljenja ostala netaknuta.

Maksimalni iznosi vertikalnih valnih momenata su za neke slučajeve oštećenja i valove u pramac znatno povećani u odnosu na neoštećen brod dok su za valove u krmu poprilično smanjeni. Stoga bi pri budućim istraživanjima bilo zanimljivo istražiti kako bi se krcanjem balasta za neke slučajeve smanjila globalna valna opterećenja i gibanja broda.

Usporedbom s rezutatima iz [21], dobivenim simulacijama u programu HydroSTAR (metodom dodane mase te metodom gubitka istisnine), primijećene su odgovarajuće razlike. Upotreba različite mreže, zadavanje trima i bočnog nagiba, zajedno s gibanjem fluida u tankovima te različite brzine napredovanja neki su od mogućih razloga tim razlikama. Za vjerodostojnije i kvalitetnije zaključke potrebna su daljnja istraživanja.

Ključne riječi: globalna valna opterećenja, brod u oštećenom stanju, gibanje krutog tijela na valovima, automatska simulacija i analiza rezultata

ABSTRACT

The present work is meant to investigate wave-induced global loads of a ship in realistic flooding conditions, while developing a code for automated hydrodynamic simulations and computation of vertical wave induced global loads.

The scenarios investigated are represented by water ingress into the starboard ballast tanks for collision damage cases and both starboard and port side tanks for grounding. Seakeeping computations are performed for 8 damage scenarios and 1 intact condition, each corresponding to different changes in displacement, trim and heel. For each of them, response amplitude operators of vertical motions are calculated using a potential linear 3D panel hydrodynamic code WAMIT in the frequency domain. The wave-induced global loads are computed using a code for post processing developed in MATLAB. The obtained results are compared with others already published.

For some cases, the results show significant variations in the global loads with respect to the intact ship.

Keywords: wave induced global loads; damaged conditions, automated simulation and post processing, rigid body motion in waves

1. INTRODUCTION

1.1. Background of the study

Rational structural design of ships should consider strength of the vessel both in intact and damage condition. Damage of merchant ship may occur due to collision with another ship, grounding or some other type of human mistake. In case of such an accident, the ship strength could be significantly reduced while still water loads may increase and could become considerable cause of the structural overloading (Luis et al. 2009 [17]). A large number of ship accidents continue to occur despite the advances with the navigation systems. These accidents cause the loss of cargo, pollution of environment, even loss of human beings. Based on statistical data of Lloyd's Register of Shipping (Lloyd's Register, 2000 [16]), a total of 1336 ships were lost with 6.6 million gross tonnage cargo loss between 1995 and 2000. 2727 people were reported killed or missing as a result of total losses in this period. So it is very important to ensure an acceptable safety level for damaged ships.

Stability is the primary effect under damage condition and almost a solved problem in the initial design of ships. In fact, there are many guidelines and rules for considering the effect of damage on stability in the preliminary design stage of various ships. The structural strength of damaged ships is the next important concern (Mohammadi et al. 2014 [18]). Conventionally, only the structural strength in intact condition was assessed in the design. Unfortunately, adequate structural strength in intact condition does not necessarily guarantee an acceptable safety margin in damaged conditions (Lee et al. 2012 [15]). Moreover, an effective damage in one section of the ship not only causes loss in structural strength of that section, but also has some effects on the other sections of the ship. Furthermore, load distribution on the ship changes depending upon the size and location of the hull damage. When a ship is damaged, the operators need to decide the immediate maintenance actions by evaluating the effects of the damage on the safety of the ship using the load prediction procedure and the residual strength assessment for the damaged ship. For these aforementioned reasons, changes in loading and structure of the ship due to damage should be considered during the design.

1.2. State of the art

Not much research has been done on wave loads of damaged ships. The main reason is that design requirements for global wave loads on damaged ship are much lower compared to the

intact condition (Hirdaris et al. 2014 [8]). Thus, the IACS Harmonized Common Structural Rules (CSR-H) (IACS, 2012 [9]), are aimed at checking the hull girder ultimate bending capacity in the damaged state using partial safety factor for wave loads of 0.67, while in the intact condition this factor reads 1.1. The reason for reduced partial safety factor in damaged condition is reduced exposure time and milder environmental conditions to be taken into account. While for intact ships the North Atlantic wave environment is usually adopted, local scatter diagrams are proposed, as applicable, for the reliability assessment of damaged ships as suggested by Luis et al. (2009) [17]. Reduced exposure time to environmental conditions after damage should also be considered before salvage to a safe location. For example, Teixeira and Guedes Soares (2010) [23] proposed a time period of one week as the voyage duration of a damaged ship to dry-dock. They concluded that the mean extreme Vertical Wave Bending Moment (VWBM) of a Suezmax tanker is about 15% lower when the exposure time is reduced from one year in the North Atlantic to one week in European coastal areas.

Although research on loads on damaged ships in waves is rare, motions of damaged ships are widely covered in the literature (e.g. Korkut et al. 2004 [13]). Application of risk-based design methods that includes structural reliability of damaged ship requires rational evaluation of all pertinent random variables, including wave loads of damaged ship (Prestileo et al. 2013 [22]) that was the motivation for some of recent studies on that subject.

Six degrees of freedom motion response tests of a Ro-Ro model have been reported in regular waves for intact and damaged conditions by Korkut et al. (2004) [13]. Korkut et al. (2005) [14] reported measurements of global loads acting on a Ro-Ro ship. The stationary model was tested in different wave heights and wave frequencies for the head, beam and stern quartering seas in order to explore the effect of damage and wave heights on the global loads acting on the model.

Chan, et al, (2001) [2] have shown that the most critical condition for a damaged Ro-Ro ship is in quartering seas. Although the vertical bending moment in quartering seas is smaller than that in head seas, the horizontal bending moment is quite large. The ratio of horizontal bending moment to vertical bending moment could be as large as 1.73. So the combined effect of vertical bending moment and horizontal bending moment is more serious. In addition, torsion, which is not considered in the above study, normally reaches maximum in quartering seas. So the effect of horizontal bending moment and torsion on the ultimate hull girder strength should be considered in the assessment of the safety level of damaged ships. If

a ship is asymmetrically flooded, some effects resulting from heel could be monitored and should be examined.

Chan et al. (2003) [1] presented wave induced load (bending moment, horizontal bending moment and dynamic torsion as well as dynamic shear force) predictions with experimental results on a damaged Ro-Ro ship using a non-linear time domain simulation method. But they did not provide more accurate results compared to those of the present linear strip method, although they applied a more complicated time domain nonlinear method.

Folso et al. (2008) [6] have performed seakeeping computations on a damaged ship by the 3D linear hydrodynamic method. The damage scenarios corresponded to water ingress into the forepeak and/ or the double hull ballast tanks of the ship sailing in full load. For the case of the flooded ballast tank in the midship area, they obtained Response Amplitude Operators (RAOs) of the VWBM larger than those evaluated for the intact condition. Interesting conclusion from the paper is that keeping a bow quartering encounter angle, with the higher freeboard on the weather side, minimizes VWBM.

Lee et al. (2012) [15] applied a computational tool based on a two dimensional linear method to predict the hydrodynamic loads of damaged warship. They obtained larger VWBM for damaged, compared to the intact ship. The global dynamic wave induced loads calculated using 2D linear method were also compared to measurements. In head and stern quartering waves, differences between computations and measurements of global dynamic wave induced load response amplitudes were reasonable.

In general, however, linear strip theory overestimated measurements for both intact and damaged ship. The analysis of wave loads on damaged ship is performed also by Downes et al. (2007) [4] where it has be shown that the RAO peak value of VWBM increases, with increasing damage size and heel angle. It can also be seen however, that there is no significant difference between the RAOs due to the effects of damage. That study indicated that the change in global hull loading may be much smaller for tankers than for Ro-Ro ferries and cruise ships.

However the previous works carried out by a number of investigators did not consider the asymmetric situations on damaged ships. This means that the vessel has to be always modelled and analysed in the upright condition without heel. The two dimensional linear suit aims at helping the operators to decide the immediate maintenance actions by evaluating the

effects of the damage and at providing acceptable predictions compared to those of a time domain simulation method [15].

When a ship is in damaged condition its floating condition could be changed dramatically. Its draught is increased and it may heel or trim. It could also have large holes in the structure. If the methodology used for intact condition is blindly applied to damaged condition, the results could be misleading. Ideally the environmental loads should be calculated together with the assessment of the residual strength of the ship.

1.3.   Aim of the study

The main goal of the thesis is to study the effect of flooded compartments on a ship regarding the global vertical loads in the presence of waves. 3D panel hydrodynamic code WAMIT is used in the analysis. WAMIT only provides numerical results for hydrodynamic coefficients and excitation as well as transfer functions of ship motion, so it is necessary to develop some tool for calculating transfer functions of wave-induced global loads along the vessel as well as for graphical presentation of results. MATLAB code is developed for calculating transfer functions of VWBM and VWSF. For graphical presentation of results, Microsoft Excel is used alongside MATLAB. After modelling the side shell of double hull oil tanker and its compartments, a MATLAB tool, able to call WAMIT to simulate the ship behavior for different flooded conditions, is developed. Transfer functions of ship motion and global wave induced loads are then calculated and plotted using tool developed in the first step.

With aim of comparison and evaluation obtained results are compared with other already published, in particular in references [20] and [21].

Analysis of results will provide relevant conclusions and indicate further work.

2. POTENTIAL FLOW THEORY AND BEHAVIOUR OF STRUCTURES IN REGULAR WAVES

2.1. Basic assumption

The sea water is assumed incompressible and inviscid. The fluid motion is irrotational. A velocity potential Φ is used to describe the fluid velocity vector $\boldsymbol{v}$ in equation (**1**) at time t at the point $\boldsymbol{x}$ (**2**) in a Cartesian coordinate system fixed in space. This means that $\mathbf{i}$, $\mathbf{j}$ and $\mathbf{k}$ are unit vectors along the x-, y- and z-axes, respectively.

$$\boldsymbol{v}(x,y,z,t) = (u,v,w)$$

$$\boldsymbol{v}(x,y,z,t) = grad\ \Phi(x,y,z;t) = \nabla\Phi = \mathbf{i}\frac{\partial\Phi}{\partial x} + \mathbf{j}\frac{\partial\Phi}{\partial y} + \mathbf{k}\frac{\partial\Phi}{\partial z} \tag{1}$$

$$\boldsymbol{x} = (x,y,z) \tag{2}$$

A velocity potential has no physical meaning itself, but is introduced because it is convenient in the mathematical analysis of irrotational fluid motion. The fluid is irrotational when the vorticity vector $\boldsymbol{\omega}$ defined in (**3**) is equal to zero everywhere in the fluid.

$$\boldsymbol{\omega} = rot\ \boldsymbol{v} = \nabla\times\boldsymbol{v} = 0 \tag{3}$$

Also, since water is incompressible velocity potential has to satisfy the Laplace equation (**4**).

$$\nabla\boldsymbol{v} = \Delta\Phi = \frac{\partial^2\Phi}{\partial x^2} + \frac{\partial^2\Phi}{\partial y^2} + \frac{\partial^2\Phi}{\partial z^2} = 0 \tag{4}$$

The complete mathematical problem of finding a velocity potential of irrotational, incompressible fluid motion consists of the solution of the Laplace equation with relevant boundary conditions on the fluid. Boundary conditions are presented in following subsections. If the z-axis it's assumed to be vertical and positive upwards, pressure p can be calculated from Bernoulli's equation (**5**) where C is an arbitrary function of time, ρ represents water density, while g denotes acceleration of gravity.

$$p + \rho gz + \rho\frac{\partial\Phi}{\partial t} + \frac{\rho}{2}\boldsymbol{v}\cdot\boldsymbol{v} = C \tag{5}$$

The time dependence of C will be included in the velocity potential and so C can be a constant. Equation (**5**) is true for unsteady, irrotational and inviscid fluid motion. It is assumed that the only external force field is gravity. Mean free-surface level corresponds to $z = 0$. The constant C can be related to the atmospheric pressure or the ambient pressure.

2.2.   Boundary conditions

For a fixed body in a moving fluid the body boundary condition on the body surface is defined as in equation (**6**) where differentiation of velocity potential along the normal to the body surface is equal to 0.

$$\frac{\partial \Phi}{\partial n} = 0 \tag{6}$$

The positive normal direction is defined to be into the fluid domain. Equation (**6**) expresses impermeability, i.e. that no fluid enters or leaves the body surface. The tangential velocity component on a body surface in a potential flow problem is unspecified. If the body is moving with velocity $\boldsymbol{u}$, equation (**6**) can be generalized as it is shown in equation (**7**).

$$\frac{\partial \Phi}{\partial n} = \boldsymbol{u} \cdot \boldsymbol{n} \tag{7}$$

Here $\boldsymbol{u}$ can be any type of body velocity. For a rigid body it includes translatory and rotary motion effects in general. This means $\boldsymbol{u}$ may be different for different points on the body surface.

A free-surface, for two dimensional flow, $v = 0$, is defined by equation (**8**) where ζ is the wave elevation.

$$z = \zeta(x, z; t) \tag{8}$$

Kinematic free-surface boundary condition, defined in equation (**9**), assumes that fluid particle on the free-surface stays on the free-surface i.e. that the vertical velocity of a water particle at the free surface of the fluid is identical to the vertical velocity of that free surface itself.

$$\frac{dz}{dt} = \frac{\partial \zeta}{\partial t} + \frac{\partial \zeta}{\partial x} \cdot \frac{dx}{dt} = \frac{\partial \zeta}{\partial t} + \frac{\partial \zeta}{\partial x} \cdot u \tag{9}$$

The dynamic free-surface boundary condition simply assumes that the water pressure is equal to the constant atmospheric pressure p_o on the free-surface. If constant C in Bernoulli's equation (**5**) is set as p_o so that the equation holds with no fluid motion for z $=\zeta$ Bernoulli's equation is transformed to (**10**) or in different notation to (**11**).

$$g\zeta + \frac{\partial \Phi}{\partial t} + \frac{1}{2}\left(\left(\frac{\partial \Phi}{\partial x}\right)^2 + \left(\frac{\partial \Phi}{\partial z}\right)^2\right) = 0 \tag{10}$$

$$g\zeta + \frac{\partial \Phi}{\partial t} + \frac{1}{2}\left(u^2 + w^2\right) = 0 \tag{11}$$

2.3. Linear wave theory

The free-surface boundary conditions (**11**) and (**10**) are non-linear. It's not known where the free-surface is before the problem has been solved. However, by linearizing the free-surface conditions one is able to simplify the problem and still get sufficient information in most cases. In the study of interactions between linear waves and linear wave-induced motions and loads on ships and offshore structures, the linear surface boundary conditions will depend on the forward speed or the presence of a current. It is assumed that the structure has no forward speed and that the current is zero. Linear theory means that the velocity potential is proportional to the wave amplitude. It is valid if the wave amplitude is small relative to a characteristic wavelength and body dimension. Linear theory transfers the free-surface conditions from the free-surface position z $= \zeta$ to the mean free-surface at $z = 0$.

The second term in expression (**9**) is a product of two values, which are both small because of the assumed small wave steepness so this product becomes even smaller (second order) and can be ignored. Linearized kinematic free-surface boundary condition at $z = 0$ is given in (**12**)

$$\frac{\partial \Phi}{\partial z} = \frac{\partial \zeta}{\partial t} \tag{12}$$

Since the waves have a small steepness (u and w are small), linearized dynamic free-surface boundary condition at $z = 0$ is given in (**13**).

$$g\zeta + \frac{\partial \Phi}{\partial t} = 0 \tag{13}$$

Equations **(12)** and **(13)** combined give combined kinematic-dynamic free-surface boundary condition stated in equation **(14)**.

$$\frac{\partial^2 \Phi}{\partial t^2} + g \frac{\partial \Phi}{\partial z} = 0 \tag{14}$$

By assuming a horizontal sea bottom and a free-surface of infinite horizontal extent one is able to derive linear wave theory (sometimes called Airy theory) for propagating waves. Sea bottom condition (no-leak condition) **(15)** defines that the vertical velocity of water particles at the sea bed, $z = -h$ is zero.

$$\frac{\partial \Phi}{\partial z} = 0 \tag{15}$$

The dynamic free-surface condition **(13)** is then used together with the Laplace equation **(4)** and the sea bottom condition **(15)** to obtain wave velocity potential given in **(16)**.

$$\Phi_w(x, z; t) = \frac{\zeta_a g}{\omega} \cdot \frac{\cosh k(h + z)}{\cosh kh} \cdot \sin(kx - \omega t) \tag{16}$$

In previous expression ζ_a represents wave amplitude, ω denotes circular wave frequency **(18)** and k denotes wave number **(19)**, while h denotes water depth. A substitution of the expression for the wave potential **(16)** in equation **(14)** gives the dispersion relation **(17)** for any arbitrary water depth.

$$\omega^2 = kg \cdot \tanh(kh) \tag{17}$$

Dispersion relation defines connection between wave frequency ω (ratio between 2π and wave period T_s) and wave number k (ratio between 2π and wavelength λ).

$$\omega = \frac{2\pi}{T_s} \tag{18}$$

$$k = \frac{2\pi}{\lambda} \tag{19}$$

2.4. Behaviour of structures in waves

Following text discusses analysis of structures in incident regular sinusoidal waves of small wave steepness. The dynamics of rigid bodies and fluid motions are governed by the

combined actions of different external forces and moments as well as by the inertia of the bodies themselves. When studying behaviour of structures in waves a steady state condition is assumed, meaning there are no transient effects present due to initial conditions. It implies that the linear dynamic motions and loads on the structure are harmonically oscillating with the same frequency as the wave loads that excite the structure [19]. The hydrodynamic problem in regular waves is normally dealt with as two sub-problems namely:

A. The forces and moments on the body when the structure is restrained from oscillating and there are incident regular waves. The hydrodynamic loads are called *wave excitation loads* and composed of so-called Froude-Kriloff and diffraction forces and moments.

B. The forces and moment on the body when the structure is forced to oscillate with the wave excitation frequency in any rigid-body motion mode. There are no incident waves. The hydrodynamic loads are identified as *added mass, damping* and <u>*restoring*</u> terms.

Due to linearity the forces obtained in A and B can be added to give the total hydrodynamic forces.

Before describing the different hydrodynamic loads, it is necessary to define a coordinate system and the rigid body motion modes. When on board a ship looking toward the bow (front end) one is looking forward. The stern is aft at the other end of the ship. As one looks forward, the starboard side is one's right and the port side is to one's left. The motions of a ship, just as for any other rigid body, can be split into three mutually perpendicular translations of the centre of gravity, G, and three rotations around G. These definitions have been visualized in Figure 1

Three translations of the ship's centre of gravity in the direction of the *x*-, *y*- and *z*-axes are:

1. surge (*x* or η_1) in the longitudinal *x*-direction, positive forwards,

2. sway (*y* or η_2) in the lateral *y*-direction, positive to port side, and

3. heave (*z* or η_3) in the vertical *z*-direction, positive upwards.

Three rotations about these axes:

1. roll (ϕ or η_4) about the x-axis, positive right turning,

2. pitch (θ or η_5) about the y-axis, positive right turning, and

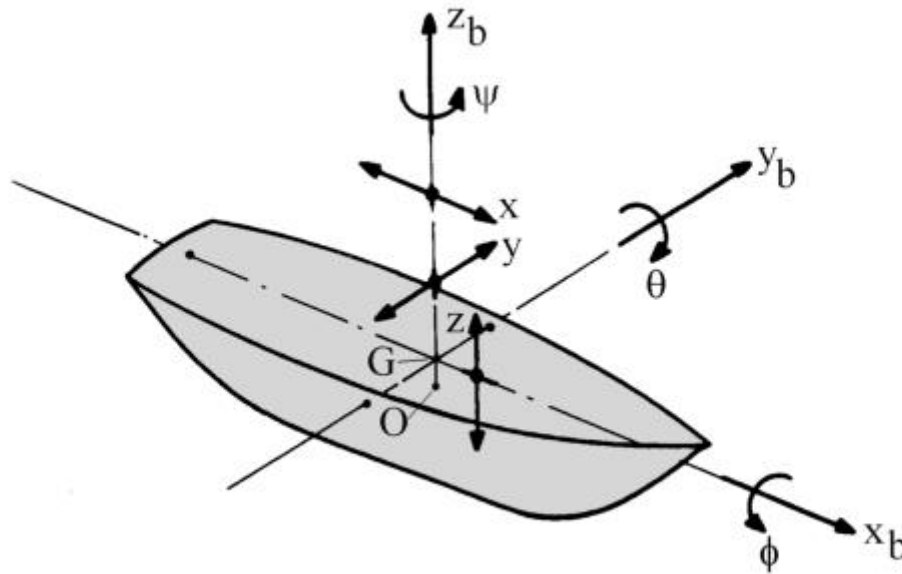3. yaw (ψ or η_6) about the z-axis, positive right turning.

Figure 1   *Definition of Ship Motions in Six Degrees of Freedom* [11].

Three right-handed orthogonal coordinate systems are used to define the ship motions:

1. **An earth-bound** coordinate system $S(x_0, y_0, z_0)$. The (x_0, y_0)-plane lies in the still water surface, the positive x_0-axis is in the direction of the wave propagation; it can be rotated at a horizontal angle μ relative to the translating axis system $O(x, y, z)$ as shown in Figure 2. The positive z_0-axis is directed upwards.

2. **A body-bound** coordinate system $G(x_b, y_b, z_b)$ is connected to the ship with its origin at the ship's centre of gravity, G. The directions of the positive axes are: x_b in the longitudinal forward direction, y_b in the lateral port side direction and z_b upwards. If the ship is floating upright in still water, the (x_b, y_b))-plane is parallel to the still water surface

3. **A steadily translating** coordinate system $O(x, y, z)$ is moving forward with a constant ship speed V. If the ship is stationary, the directions of the $O(x, y, z)$ axes are the same as those of the $G(x_b, y_b, z_b)$ axes. The (x, y)-plane lies in the still water surface with the origin 0 at, above or under the time-averaged position of the centre of gravity G. The ship is supposed to carry out oscillations around this steadily translating $O(x, y, z)$ coordinate system.
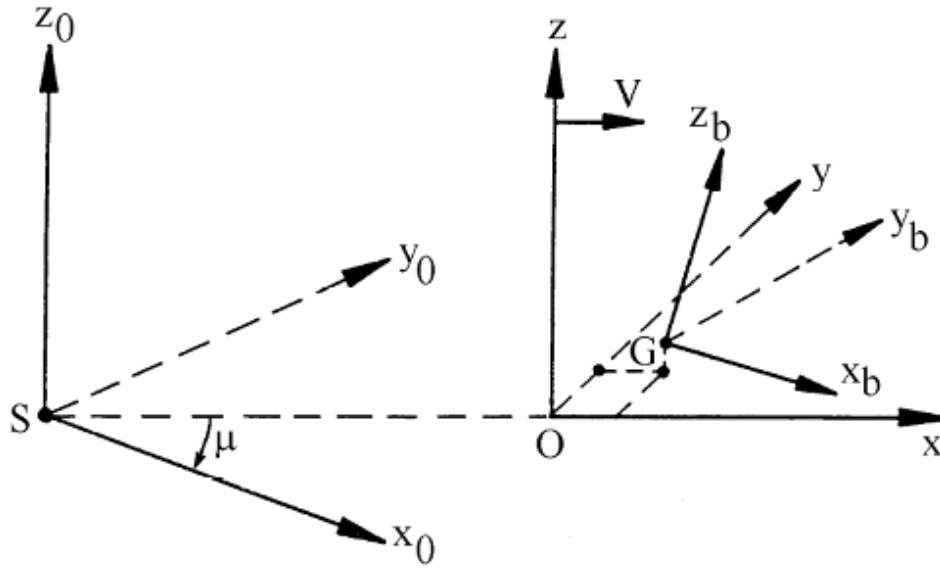
Figure 2 *Coordinate systems* [11].

Knowing the motions of and about the centre of gravity, G, one can calculate the motions at any point on the structure using superposition. Absolute motions are the motions of the ship in the steadily translating coordinate system O(x, y, z). The angles of rotation η_4, η_5 and η_6 are assumed to be small because it is a necessity for linearization. Absolute harmonic motions of a certain point $P(x_P, y_P, z_P)$ on the structure are given by equation (**20**).

$$x_P = \eta_1 - y_b\eta_6 + z_b\eta_5$$

$$y_P = \eta_2 + x_b\eta_6 - z_b\eta_4 \qquad (20)$$

$$z_P = \eta_3 - x_b\eta_5 + y_b\eta_4$$

As is already said flow around the structure in regular wave is described by total velocity potential. The linearization of the problem permits the decomposition of the total velocity potential Φ into the radiation Φ_R and diffraction Φ_D components as in (**22**).

$$\Phi(x, y, z; t) = \Phi_D(x, y, z; t) + \Phi_R(x, y, z; t) \qquad (21)$$

Diffraction potential Φ_D is used to describe flow around the structure restrained from oscillating that occurs due to incident regular waves.

$$\Phi_D(x, y, z; t) = \Phi_0(x, y, z; t) + \Phi_7(x, y, z; t) \qquad (22)$$

As equation **(22)** denotes diffraction potential Φ_D is composed from the incident wave velocity potential Φ_0 and the velocity potential Φ_7 due to scattered disturbance of the incident wave by the body fixed at its undisturbed position. Incident wave velocity potential Φ_0 for 3D flow in complex notation is given in equation **(23)**, where β is the angle between the direction of propagation of the incident wave and the positive x-axis as defined in Figure 3.

$$\Phi_0(x,y,z;t) = \frac{ig\zeta_a}{\omega} \cdot \frac{\cosh[k(h+z)]}{\cosh(kh)} \cdot e^{-ikx\cos\beta - iky\sin\beta + i\omega t} \qquad (23)$$

Radiation potential Φ_R is used to describe flow around the structure that is forced to oscillate with the wave excitation frequency in any rigid-body motion mode.

$$\Phi_R(x,y,z;t) = i\omega \sum_{j=1}^{6} \zeta_j \Phi_j \qquad (24)$$

The constants ζ_i denote the complex amplitudes of the body oscillatory motion in its six rigid-body degrees of freedom, while Φ_j represents the corresponding unit-amplitude radiation potential.

On the undisturbed position of the body boundary, the radiation and diffraction potentials are subject to the no-leak boundary conditions:

$$\frac{\partial \Phi_7}{\partial n} = -\frac{\partial \Phi_0}{\partial n} \qquad (25)$$

$$\frac{\partial \Phi_j}{\partial n} = v_{n,i} \qquad (26)$$

Under the assumptions that the responses are linear and harmonic, the equation of motions of a vessel in regular waves can be written in the following general equation of coupled motions.

$$\left([M_{ij}] + [A_{ij}]\right)\{\ddot{\eta}_j\} + [B_{ij}]\{\dot{\eta}_j\} + [C_{ij}]\{\eta_j\} = \{F_i\} \qquad (27)$$

In previous expression $[M_{ij}]$ represents generalised mass matrix, $[C_{ij}]$ denotes matrix of hydrostatic and gravitational restoring coefficients, $\{F_i\}$ denotes vector of exciting forces and moments, $[A_{ij}]$ and $[B_{ij}]$ are matrices of the added mass and damping coefficients, while j and k indicate the direction of fluid force and the modes of motion (i, j = 1-surge, 2-sway, 3-

heave, 4-roll, 5-pitch, 6-yaw).Computation of hydrodynamic and hydrostatic coefficients and forces is presented in 2.5.
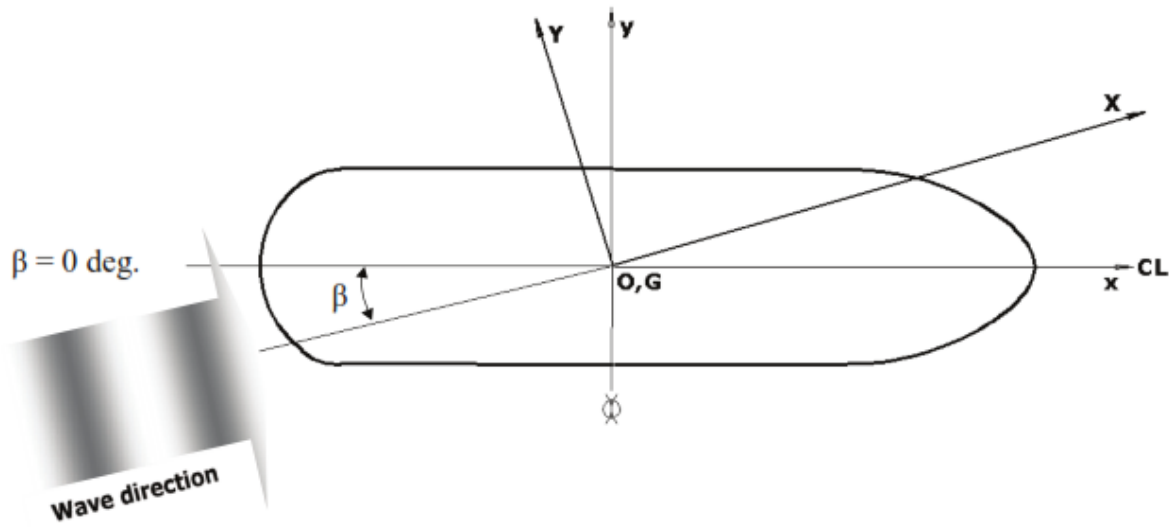

Figure 3   *Definition of wave heading* [15].

2.5. Hydrodynamic and hydrostatic quantities evaluated by WAMIT

Body motions and forces are defined in relation to the origin of the same Cartesian coordinate system relative to which the panel offsets are defined. Note that this origin may be located on, above or below the free surface.

2.5.1. Hydrostatic data

All hydrostatic data can be expressed in the form of surface integrals over the mean body wetted surface S_b, by virtue of Gauss' divergence theorem. All three forms of the displacement volume ∇ are devaluated in WAMIT, as independent checks of the panel coordinates. The median volume of the three is used for the internal computations.

$$\nabla = -\iint_{S_b} n_1 x \, dS = -\iint_{S_b} n_2 y \, dS = -\iint_{S_b} n_3 z \, dS \tag{28}$$

Coordinates of center of buoyancy are calculated from **(29)**.

$$x_b = \frac{-1}{2\nabla} \iint_{S_b} n_1 x^2 \, dS$$

$$\tag{29}$$

$$y_b = \frac{-1}{2\nabla} \iint_{S_b} n_2 y^2 \, dS$$

$$z_b = \frac{-1}{2\nabla} \iint_{S_b} n_2 z^2 \, dS$$

Matrix of hydrostatic and gravitational restoring coefficients $[C_{ij}]$ is defined in **(30)** and **(31)**, where $C(i, j) = C(j, i)$ for all i, j, except for $C(4, 6)$ and $C(5, 6)$. For all other values of the indices i, j, $C(i, j) = 0$. In particular, $C(6, 4) = C(6, 5) = 0$.

$$C(3,3) = \rho g \iint_{S_b} n_3 \, dS$$

$$C(4,4) = \rho g \iint_{S_b} y^2 n_3 \, dS + \rho g \nabla z_b - m g z_g \qquad \text{(30)}$$

$$C(5,5) = \rho g \iint_{S_b} x^2 n_3 \, dS + \rho g \nabla z_b - m g z_g$$

$$C(3,4) = \rho g \iint_{S_b} y n_3 \, dS$$

$$C(3,5) = -\rho g \iint_{S_b} x n_3 \, dS$$

$$C(4,5) = -\rho g \iint_{S_b} x y n_3 \, dS \qquad \text{(31)}$$

$$C(4,6) = -\rho g \nabla x_b + m g x_g$$

$$C(5,6) = -\rho g \nabla y_b + m g y_g$$

In $C(4,4)$, $C(4,6)$, $C(5,5)$ and $C(5,6)$, m denotes the body mass, while (x_g, y_g, z_g) represent coordinates of the center of gravity.

2.5.2. Hydrodynamic data

Added-mass and damping coefficient are obtained from equation

$$A_{ij} - \frac{i}{\omega} B_{ij} = -\rho \iint_{S_b} n_i \Phi_j \, dS \qquad \text{(32)}$$

Exciting forces and moments are obtained from direct integration of hydrodynamic pressure:

$$F_i = -i\omega\rho \iint_{S_b} n_i \Phi_D \, dS \tag{33}$$

The complex unsteady hydrodynamic pressure on the body boundary or in the fluid domain is related to the velocity potential (21) by the linearized Bernoulli equation (5) which leads to expression (34).

$$p = -\rho \frac{\partial \Phi}{\partial t} \tag{34}$$

2.5.3. Body motion in waves

The inertia matrix is defined as follows.

$$M = \begin{bmatrix} m & 0 & 0 & 0 & mz_g & -my_g \\ 0 & m & 0 & -mz_g & 0 & mx_g \\ 0 & 0 & m & my_g & -mx_g & 0 \\ 0 & -mz_g & my_g & I_{11} & I_{12} & I_{13} \\ mz_g & 0 & -mx_g & I_{21} & I_{22} & I_{23} \\ -my_g & mx_g & 0 & I_{31} & I_{32} & I_{33} \end{bmatrix} \tag{35}$$

The moments of inertia I_{ij} are defined in terms of the corresponding radii of gyration r_{ij}, defined by the relation (36).

$$I_{ij} = mr_{ij}^2 \tag{36}$$

The complex amplitudes of the body's motions are obtained from the solution of the 6×6 linear system (37).

$$\sum_{j=1}^{6} \left[-\omega^2 (M_{ij} + A_{ij}) + i\omega B_{ij} + C_{ij} \right] \zeta_j = F_i \tag{37}$$

Ratio between ship response and wave amplitude is expressed by response amplitude operator *RAO*.

$$RAO_j = \frac{\zeta_j}{\zeta_a} \tag{38}$$

3. COMPUTATIONAL ASPECTS

3.1.   Software adopted for computations

WAMIT (Wave Analysis at Massachusetts Institute of Technology) is a radiation/diffraction program based on a three-dimensional panel method, following the potential theory developed for the analysis of the interaction of surface waves with offshore structures. The main program consists of two top-level sub-programs POTEN and FORCE which evaluate the velocity potentials and desired hydrodynamic parameters, respectively. The water depth can be infinite or finite, and either one or multiple interacting bodies can be analysed. The bodies may be located on the free surface, submerged, or mounted on the sea bottom. A variety of options permit the dynamic analysis of bodies which are freely floating, restrained, or fixed in position.

The flow is assumed to be ideal and time-harmonic. The free-surface condition is linearized (except in Version 6.1S where the second-order free-surface condition and body boundary conditions are imposed). We refer to this as the 'linear' or 'first-order' analysis.

Mean second-order forces are included in this analysis, since they can be computed rigorously from the linear solution. The radiation and diffraction velocity potentials on the body wetted surface are determined from the solution of an integral equation obtained by using Green's theorem with the free-surface source-potential as the Green function.

WAMIT is designed to be flexible in its use with a variety of practical applications. It consists of two subprograms, POTEN and FORCE, which normally are run sequentially. POTEN solves for the radiation and diffraction velocity potentials (and source strengths) on the body surface for the specified modes, frequencies and wave headings. FORCE computes global quantities including the hydrodynamic coefficients, motions, and also first and second-order forces. Velocities and pressures on the body surface are evaluated by FORCE. Additional field data may also be evaluated by FORCE, including velocities and pressures at specified positions in the fluid domain and wave elevations on the free surface.

Except WAMIT, MATLAB is used for developing codes for calling WAMIT simulations automatically and post-processing of obtained numerical data. MATLAB (matrix laboratory) is a multi-paradigm numerical computing environment and fourth-generation programming language. MATLAB allows matrix manipulations, plotting of functions and data,

implementation of algorithms, creation of user interfaces, and interfacing with programs written in other languages.

3.2. Adopted mesh and damaged vessel scenarios

The studied ship is Aframax oil tanker with main particulars presented in Table 1. Cargo hold area is divided into 6 pairs of Cargo Tanks (CT) and 6 corresponding pairs of Water Ballast Tanks (WBT) in double bottom and side. WBTs are divided into portside and starboard tanks by center line girder in double bottom. The general arrangement of the ship is shown in Figure 4. The damage scenarios correspond to water ingress into the double hull ballast tanks of the ship sailing in full load. From a computational point of view, the simulated amount of water entries corresponds to static equilibrium situations where internal levels in the compartments affected by the flooding are equal to the still water external levels.

Table 1   *Main particulars of the Aframax oil tanker.*

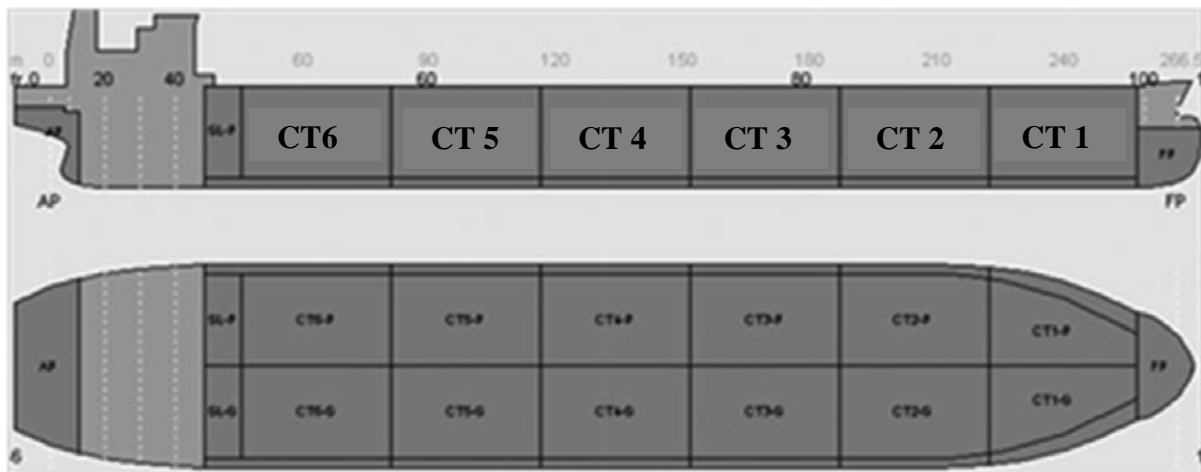| Dimension	Unit (m, dwt)
Length between perp., L_{PP}	234
Breadth, B	40
Depth, D	20
Draught, T	15
Deadweight, DWT	105000

Figure 4   *General arrangement of the Aframax oil tanker.*

Side shell of double hull oil tanker and its compartments are created in 3D computer graphics and computer-aided design (CAD) application software Rhinoceros (Rhino3D). Discretization of the hull i.e. meshing is based on a distribution of plane quadrilaterals, hereafter denoted simply as panels. Panels usually do not require to be connected i.e. hanging nodes and small

gaps in the mesh are possible without compromising the validity of the obtained results Jafaryeganeh et al. (2014) [7].
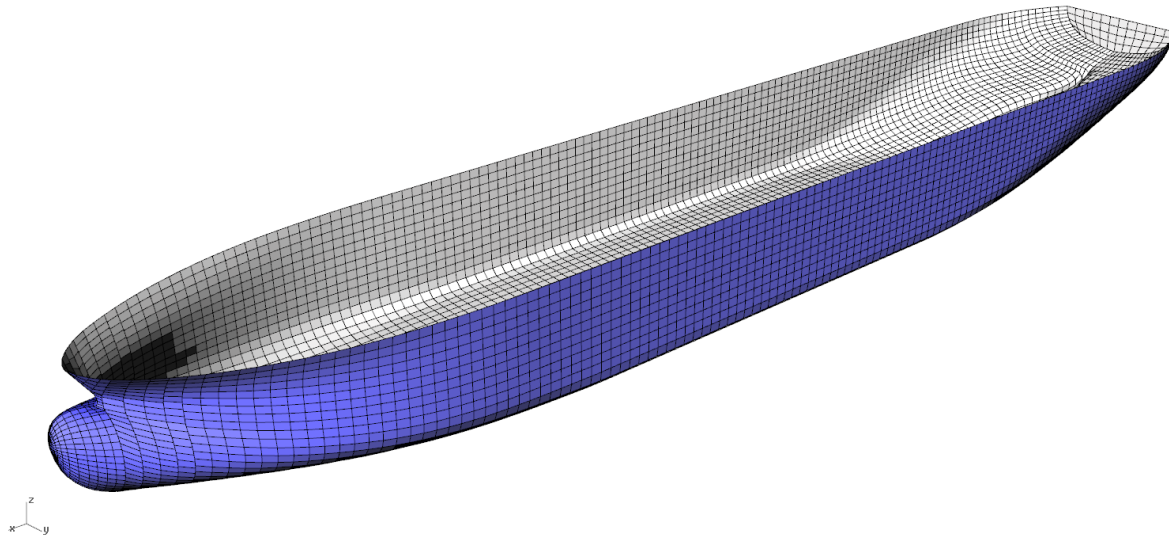

Figure 5   *Hydrodynamic panel model of the intact tanker.*

Ko et al. (2011) [12] relate the required panel size to depend on the incident wave length, and so does DNV (2010). The latter gives a set of general directives regarding the panels: diagonal length less than 1/6 of the shortest wave length analysed; refined mesh in the areas of abrupt geometrical change; and increased refinement of the mesh in the vicinity of the waterline.
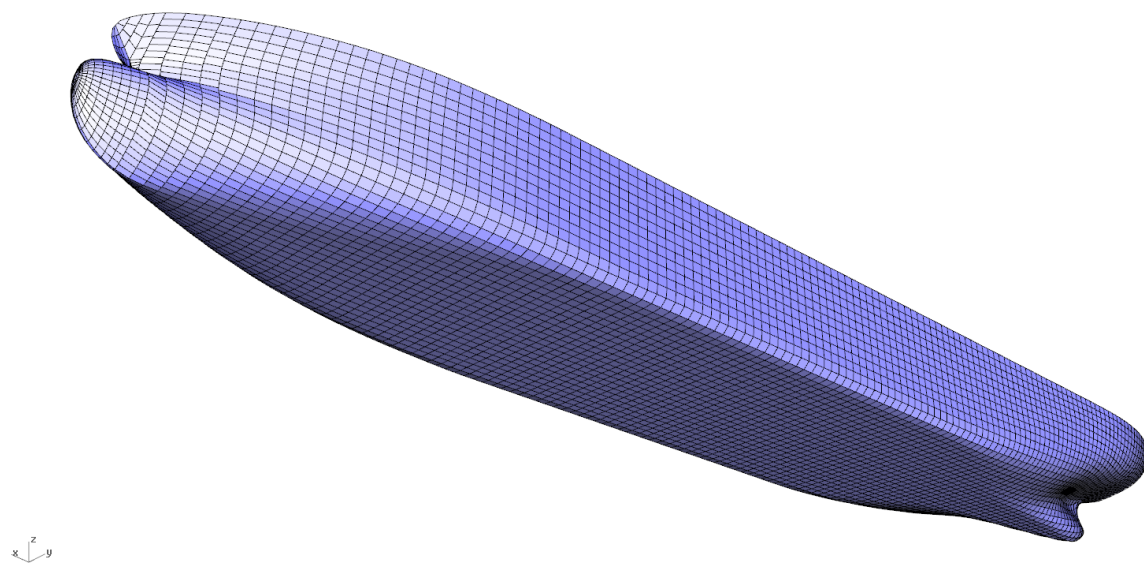

Figure 6   *Hydrodynamic panel model of the intact tanker (bottom view).*

Due to lack of time, sensitivity tests haven't been carried out so panels' size are defined respecting previously mentioned directives form DNV. The hydrodynamic panel model of the intact ship presented in Figure 5 and Figure 6. Wetted hull surface of the intact tanker is modelled with 6698 panels. For other cases number of panels varies depending on number of damaged tanks each having around 800 panels. Figure 7 presents hydrodynamic panel model of starboard side (SB) WBTs no. 1, 4, and 6.
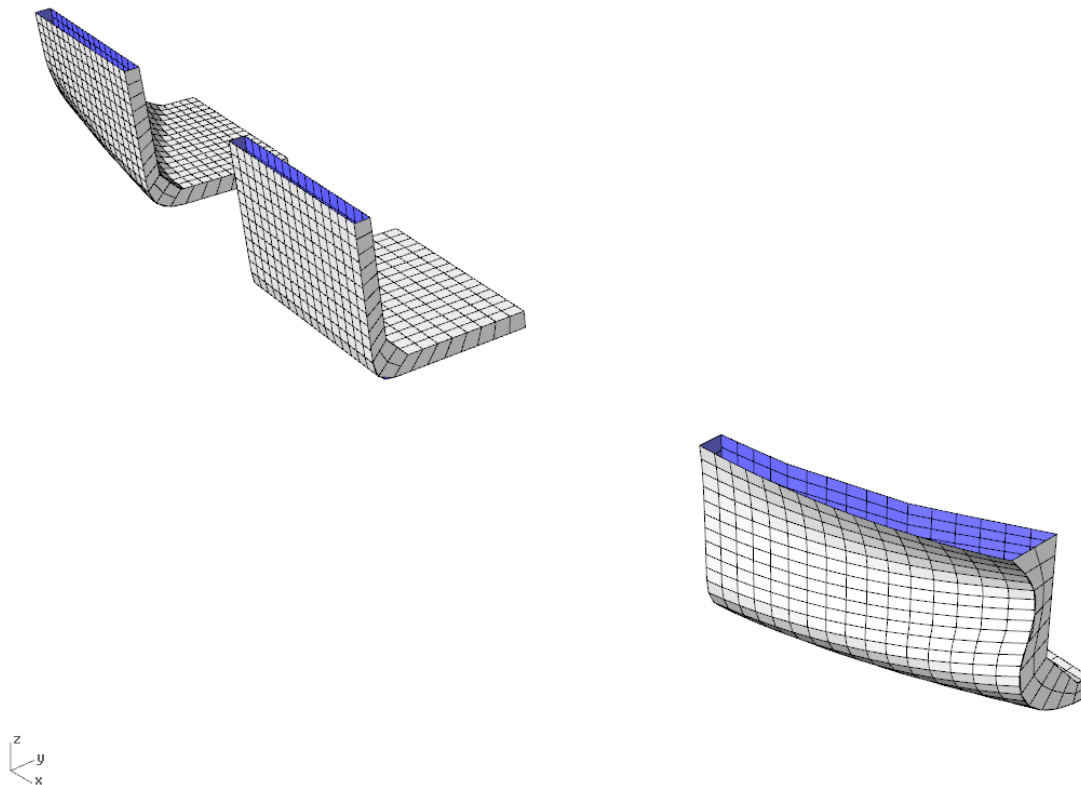

Figure 7   *Hydrodynamic panel model of the WBTs nos. 1, 4 and 6.*

As ship damage may occur in a number of ways, damage parameters are in general random quantities that may be described by probability distributions. Such probability distributions of damage size and location, for cases of the collision and grounding damages are proposed by International Maritime Organization (IMO, 2003). In order to define credible damage scenarios, Monte Carlo (MC) simulation according to IMO probabilistic models is performed by Parunov et al. (2015) [21]. 1000 random numbers are drawn according to IMO models and events resulting in damage of certain number of compartments counted and presented in Figure 8 a) and b) for collision and grounding respectively. Figure 8 shows probabilities of damage in the longitudinal sense only, i.e. it is assumed that only WBTs are damaged, while

damage does not penetrate through the inner bottom or inner hull. Fore peak tank and engine room are also considered as separate tanks in the present damage analysis.
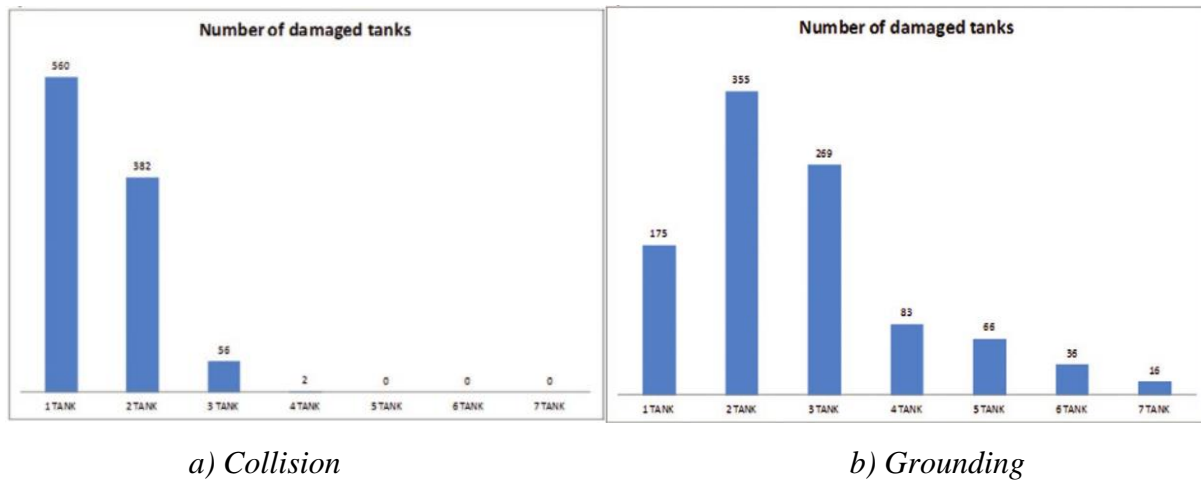

<div align="center">

a) Collision   *b) Grounding*

</div>

Figure 8   *Probabilities of number of damaged tanks in the longitudinal direction Values represent number of outcomes in 1000 simulations* [21].

Single tank damage in Figure 8 represents case when outcome of MC simulation results in the damage of only one of WBTs or FP tank or engine room. Two tanks damage case means that MC simulation results in the damage of FP tank and WBT no.1, any combination of two consecutive WBTs or WBT no.6 and the engine room. For damage of more tanks applies analogous reasoning is applied. Furthermore, it is to be noted that the collision always results in the asymmetrical damage, i.e. only starboard or portside tanks are damaged. For grounding, however, damage may be symmetrical, i.e. pairs of WBTs may be damaged together. Such conservative assumption is adopted in the present study, i.e. grounding damage is considered always as symmetrical damage. It is interesting to notice from Figure 3 that damage of single compartment has the highest probability for collision, while damage of two pairs of compartments is the most probable scenario for grounding.

The scenarios investigated are represented by water ingress into the starboard ballast tanks for collision damage cases and both starboard and port side tanks for grounding as presented in Table 2. In total, 9 damage cases including intact condition are examined. Grounding damage cases, precisely 2 of them are studied mainly for comparison with previous work presented in Parunov et al 2015 [21] and obtaining some rough validation. Furthermore 6 collision damage cases are also presented in the thesis.

The linear approximation in 3D potential flow simulations applied to cases presented in Table 2 is questionable, as the inclination and trim of the vessel adds nonlinear aspects to the problem. This applies in particular (but not only) to the hydrostatic restoring terms for

vertical, pitch and roll motions. In the examined cases, the ship sides are actually inclined with respect to the free surface; this results in reality in a lateral and longitudinal displacement of the centre of buoyancy creating an evident dissymmetry in the restoring forces for listed motions and a coupling between the motions in the longitudinal and transversal planes.

Table 2   *Intact and damaged conditions details.*

Damage case	Damaged tanks	Draught (m)	Trim (°)	Heal (°)
DC0 (intact)	NONE	15.00	0	0
DC 1	WBT: 2S	15.99	0.65	1.71
DC 2	WBT: 3S	15.98	0.39	2.30
DC 3	WBT: 4S	15.99	0.16	2.54
DC 4	WBT: 1S+2S	16.28	0.89	3.73
DC 5	WBT: 3S+4S	16.26	0.52	4.26
DC 6	WBT: 5S+6S	16.25	0.08	4.44
DC 7	WBT: 4P&S	16.23	0.43	0.24
DC 8	WBT: 2-4P&S	17.36	1.13	0.22

3.3. WAMIT files

For better understanding of ideas and procedures in MATLAB codes it is necessary to become familiar with WAMIT input and output files. Five input files are used for simulations presented in this thesis:

- Filenames list (FNAMES.WAM) is used to specify the filenames of the primary input files CFG, POT, FRC, and GDF

- Configuration file (*.cfg) is used to specify various parameters and options in WAMIT

- Geometric Data File (*.gdf) is used for specific body geometry mesh data

- Potential Control File (*.pot) is used to specify various parameters for POTEN subprogram:

  o water depth h,

  o wave periods T_s or frequencies ω,

  o wave heading angle β,

o   motions included in simulation and

o   position of body-fixed coordinate system relative to the global coordinate system

- Force Control File (*.frc) is used to specify various parameters for FORCE subprogram:

  o   which hydrodynamic parameters are to be evaluated and output from the program,

  o   fluid density ρ,

  o   coordinates of the body center of gravity,

  o   the inertia matrix as defined in **(35)** and so on

Output files used for post-processing are:

- Low-order GDF file (*_low.gdf) - from input GDF file WAMIT creates body surface mesh up to waterline using flat quadrilaterals.

- Numeric output files (*.*num*) created for each hydrodynamic parameter evaluated in the FORCE subprogram.

Detailed description of listed files is given in WAMIT User manual Version 6.4 [25].

3.4.   MATLAB codes

Three separate codes have been created in MATLAB for the purpose of this research. Created tools cooperate with WAMIT and are able to create input files, run simulations and collect data, as well to calculate wave induced loads during post-processing faze for a lot of different damage scenarios.

A lot of data modification and transfer algorithms are included in the codes so it would be time and paper consuming if every code line were explained. Instead only main ideas and mathematical background of computations are presented in this thesis.

3.4.1.   MATLAB code for automated creation of input files and running of simulations in WAMIT

Before running simulations, for each damage scenario it is necessary to create input files. For each damage scenario, folder along with corresponding input files is created. Information for creating input files, along with data about damage cases and ship in particular are imported

from specifically defined excel file. Along with data from Table 2 and Table 3 that file also contains necessary inertia matrix information: body mass, coordinates of the center of gravity and moments of inertia. Actual code has around 400 lines so thereby highly simplified version of pseudocode is given in following 12 lines.

```
1- Import path          % location of folder with input files for this code
2- Export path          % location of folder with output files and folders
3- Import data from excel file
```

Variables in 1st line, as it stated in comment, define location of folder that contains input files for presented code. Location of folder containing output files and folders that are actually input files for WAMIT is defined in 2nd line. Line 3 represents data import from excel file and assignment to respective variables. Loop from 4th to 12th line creates WAMIT input files for each damage case.

```
% automated creation of input files, i represents specific damage case (DC)
4- for i = 1 to nDC              % nDC denotes number of damage cases
5-    create folder (fname(i))   % function that creates folder for WAMIT
                                   input files for specified DC
6-    create file (FNAMES.WAM)   % function that creates file FNAMES.WAM
7-    create file (fname(i).pot) % function that creates POT file
8-    create file (fname(i).frc) % function that creates FRC file
9-    create file (fname(i).gdf) % function that creates GDF file
10-   create file (fname(i).cfg) % function that creates CFG file
11-   save files

12-   end
```

Folder for saving WAMIT input files for each damage case (DC) is created in line 5. Variable `fname(i)` denotes file name for every DC while `i` represents number of damage case. Filenames list (FNAMES.WAM) contains names of other 4 input files so only number that indicates DC in file names is changed for each pass through loop. Except line that indicates GDF file for simulation, data in POT file remains unchanged for different damage cases. In FRC file only distance between vertical centre of gravity (VCG) and reference coordinate system placed on waterline, z_{gi}, has to be changed. Draught for specific DC (T_i) is listed in Table 2.

$$z_{gi} = VCG - T_i \tag{39}$$

GDF file for specific damage case (DC) is created combining intact ship hull GDF file with particular GDF file of WBT plating. Those files are located in input folder defined in 1st line. Table 3 contains information which GDF files are relevant for specific DC.

Table 3   *Instructions for creating GDF files.*

DC	Damaged tanks	No. of d.t.	WBT 1S = 1	WBT 2S = 2	WBT 3S = 3	WBT 4S = 4	WBT 5S = 5	WBT 6S = 6	WBT 1P = 7	WBT 2P = 8	WBT 3P = 9	WBT 4P = 10	WBT 5P = 11	WBT 6P = 12
1	WBT: 1S	1	2											
2	WBT: 4S	1	3											
3	WBT: 6S	1	4											
4	WBT: 1S+2S	2	1	2										
5	WBT: 3S+4S	2	3	4										
6	WBT: 5S+6S	2	5	6										
7	WBT: 4P&S	2	4	10										
8	WBT: 2-4P&S	6	2	3	4	8	9	10						

There are 12 WBT, so numbers from 1 to 12 are assigned to each tank starting from starboard WBT at bow, as it is shown in bolded part of Table 3. For each damage case is necessary to define number of damaged tanks (3rd column) and in following columns numbers that define damaged tanks. Damage case 7 e.g. has 2 damaged tanks and numbers 4 and 10 are listed in table that indicates that WBT 4S and 4P GDF files are to be merged with intact hull GDF file. Merging of files is done using for loop that goes from 1 to number of damage tanks. With every pass through the loop panels from WBT GDF file are copied to GDF for considered DC that, before entering loop, contains only panels from the ship hull. After DC GDF file is created. In CFG file, only data for heel and trim (listed in Table 2) angle has to be changed. Free surface water level in internal tanks is set to correspond to waterline free surface around the hull. At the end of each loop created files for specific DC are saved to folder defined in 5th line.

After input files are created code for automated calling of WAMIT is run. It is a short code containing only functions for moving files and calling WAMIT executable file. Pseudocode is given in following lines.

```
1- move files (input files)
2- run(wamitv6.4.exe)
3- move files (output files)
```

Function in 1st line, transfers input files from DC folder (`fname(i)`) to folder containing WAMIT executable file. After the simulation is finished output files are transferred, by function in 3rd line, back into same DC folder.

For post-processing obtained results MATLAB code for calculation of wave induced loading is developed and short description is given in following subsection.

3.4.2. MATLAB code for calculation of wave induced loading

As already noted WAMIT doesn't provide numerical results for wave-induced global loads along the vessel and therefore MATLAB code has been developed to address that issue. MATLAB code contains more than a 1000 lines so only mathematical background and main idea are to be explained.

The total structural loading at any instant is a sum of the wave pressure forces, the ship motion-induced pressure forces and the reaction loads due to the acceleration of the ship masses. Calculation of bending moment and shear force on a ship hull in waves requires knowledge of the time-varying distribution of fluid forces over the wetted surface of the hull $f(x)$ together with the distribution of the inertial reaction loads $m(x)a_z(x)$. Fluid loads depend on the wave-induced motions of the water and the corresponding motions of the ship. The inertial loads are equal to the product of the local mass of the ship $m(x)$ and the local absolute acceleration $a_z(x)$. The shear force V and bending moment M are then obtained at any instant by evaluating the first and second integrals of the longitudinally distributed net vertical force per unit length $q(x)$ defined in equation **(40)**.

$$q(x) = f(x) + m(x)a_z(x) \tag{40}$$

At any instant of time, the shear force, $V(x_1)$, at a section whose x-coordinate is x_1 is obtained by integrating $q(x)$ from the aft end of the ship, $x = 0$, up to the station at $x = x_1$. The bending moment $M(x_1)$ at x_1, is obtained, in turn, by integrating the shear force, $V(x)$, from $x = 0$ to $x = x_1$.

$$V(x_1) = \int_0^{x_1} q(x)dx \tag{41}$$

$$M(x_1) = \int_0^{x_1} V(x)dx = \int_0^{x_1}\int_0^{x_1} q(x)dx\,dx \tag{42}$$

In order to compute integrals, ship hull along with mass is discretized into a series of transverse strips of constant length of 1.92m. One of the important assumptions of linear strip theory is that both the wave and ship motion amplitudes are, in some sense, small. As a result, it is possible to consider the total instantaneous vertical fluid force $f(x)dx$ on a thin transverse strip or element of length, dx, to be composed of the sum of several terms that are computed independently of each other. Corresponding with WAMIT outputs, vertical fluid force $f(x)dx$ is decomposed in to hydrodynamic pressure force $f_{hp}(x)dx$ and restoring force $f_r(x)dx$.

$$f(x)dx = f_{hp}(x)dx + f_r(x)dx \tag{43}$$

Vertical hydrodynamic pressure panel force $f_{hp}(x)dx$, is calculated by multiplying the pressure acting on the surface of the panel p_i, defined in expression **(34)**, panel surface $A_{p,i}$ and z-component of panel surface normal vector $n_{3,i}$. Vertical hydrodynamic pressure force for specified strip is computed summing $f_{hp,i}(x)dx$ for all panels along specified strip, N_{sp}.

$$f_{hp}(x)dx = \sum_{i=1}^{N_{sp}} p_i A_{p,i} n_{3,i} \tag{44}$$

For an arbitrary quadrilateral $V_0V_1V_2V_3$ one can take the midpoints of its 4 edges to get 4 vertices which form a new quadrilateral $M_0M_1M_2M_3$ as presented in. Figure 9. It is then easy to show that this midpoint quadrilateral is always a parallelogram, called the "Varignon parallelogram", and that its area is exactly one-half the area of the original quadrilateral [26]. Area of quadrilateral $V_0V_1V_2V_3$ can be computed using expression **(45)**. Panel normal vector is obtained by normalizing cross product of vector V_2V_0 and vector V_3V_0.
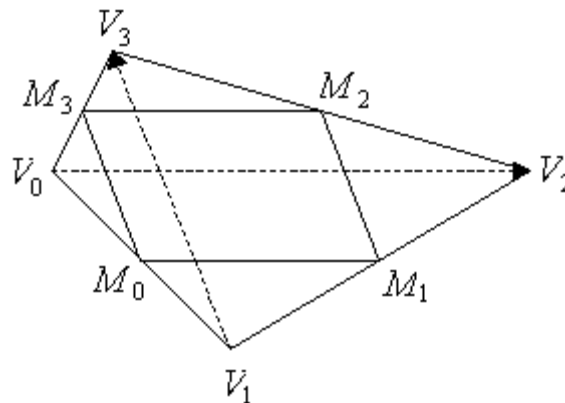
Figure 9   *Arbitrary quadrilateral* [26].

$$A_{p,i} = 2|M_0 M_1 M_2 M_3| = 2\left|\left(\frac{V_1 + V_2}{2} - \frac{V_0 + V_1}{2}\right) \times \left(\frac{V_3 + V_0}{2} - \frac{V_0 + V_1}{2}\right)\right|$$
$$= \frac{1}{2}|(V_2 - V_0) \times (V_3 - V_1)|$$

(45)

To simplify sorting of panels and computation of hydrodynamic force $f_{hp}(x)dx$ on a strip, size and distribution of panels are taken into a consideration while creating a mesh. Maximum panel length correspond to strips length, while whole surface of the panel has to be inside one strip only. In Figure 10, a closer look on mesh is presented and one can see that panels are sorted vertically forming strips and facilitating numerical integration.
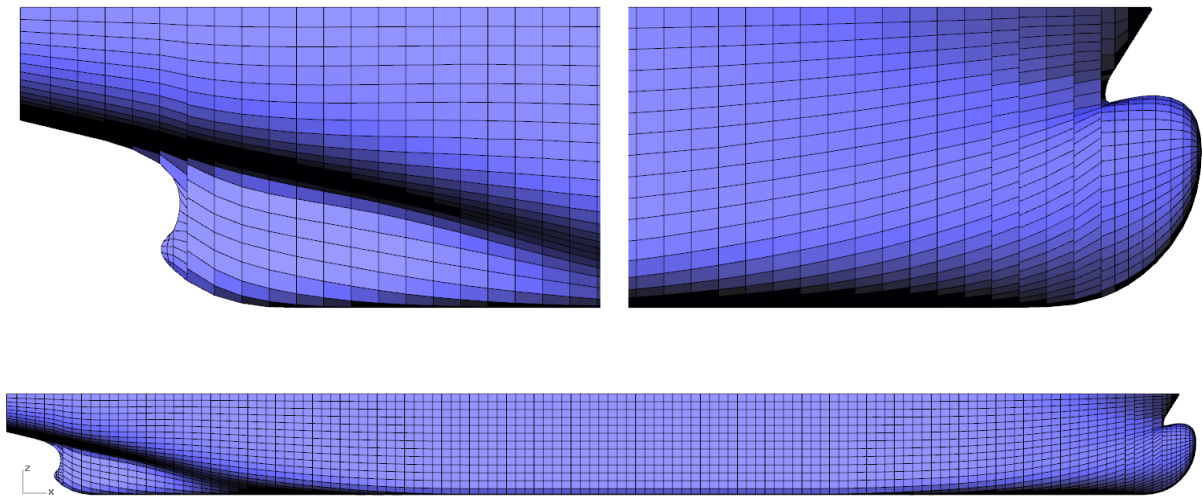
Figure 10 *Closer look on mesh definition.*

Restoring force is defined in equation **(46)** where $B_{wl}(x)$ denotes beam of a strip on waterline.

$$f_r(x)dx = \rho g B_{wl}(x)dx$$

(46)

Local mass of the ship $m(x)$ is obtained from input excel file with predefined mass distribution. At any instant of time, the motion of the ship will consist of superimposed motions of pitch and heave, so $a_z(x)$ is calculated from equation **(47)**, where RAO_3 represents response amplitude operator of heave motion while RAO_5 denotes response amplitude operator of pitch motion.

$$a_z(x) = -\omega^2(RAO_3 + xRAO_5)$$

(47)

4. RESULTS

RAOs of VWBM at amidships and RAOs of heave and pitch motions are calculated for intact and for damaged ship conditions. RAOs of VWBM for damaged vessel are determined for 8 damage cases. As for the computation of ship motions, ship speed is assumed to be zero. Two grounding damage cases are used for comparative analysis of loads and motions. Is should be emphasized that there are some differences between model used in WAMIT and one used in HydroSTAR i.e. mesh used for simulation is not completely the same and the HydroSTAR simulations for damage cases are run with speed of advance equal to 5 knots.

4.1.   Comparison between ship motions calculated by WAMIT and HydroSTAR

Results of the comparative analysis of heave motion for intact case are presented in Figure 11, 12 and 13.
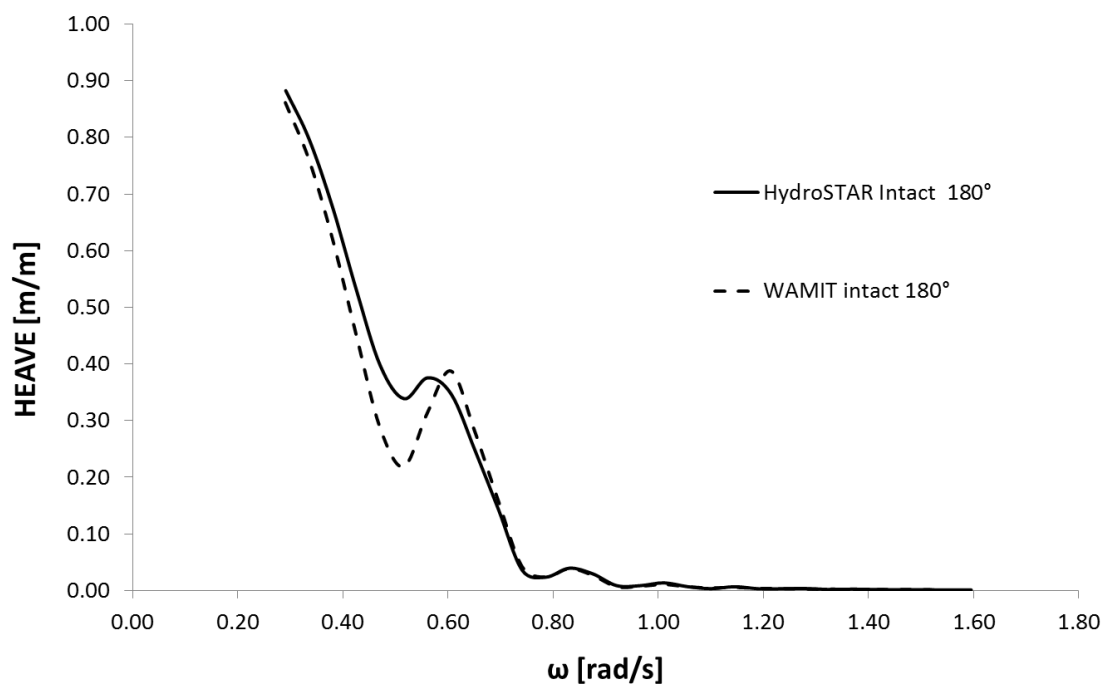
Figure 11 *RAOs of heave motion for head seas.*
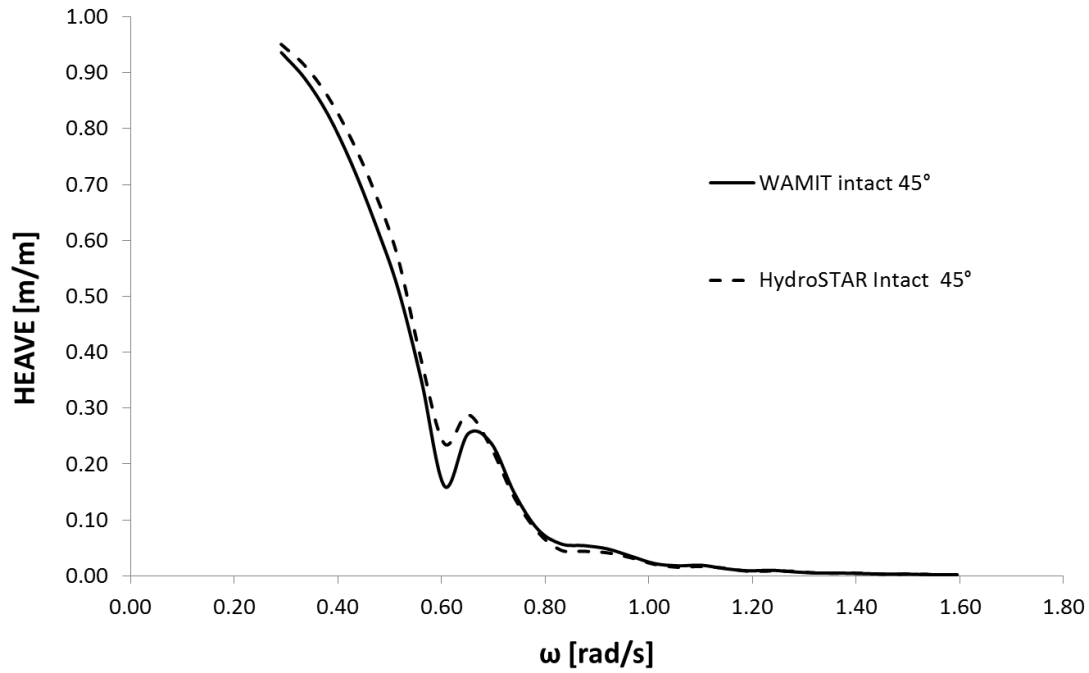
Figure 12 *RAOs of heave motion for quartering seas.*
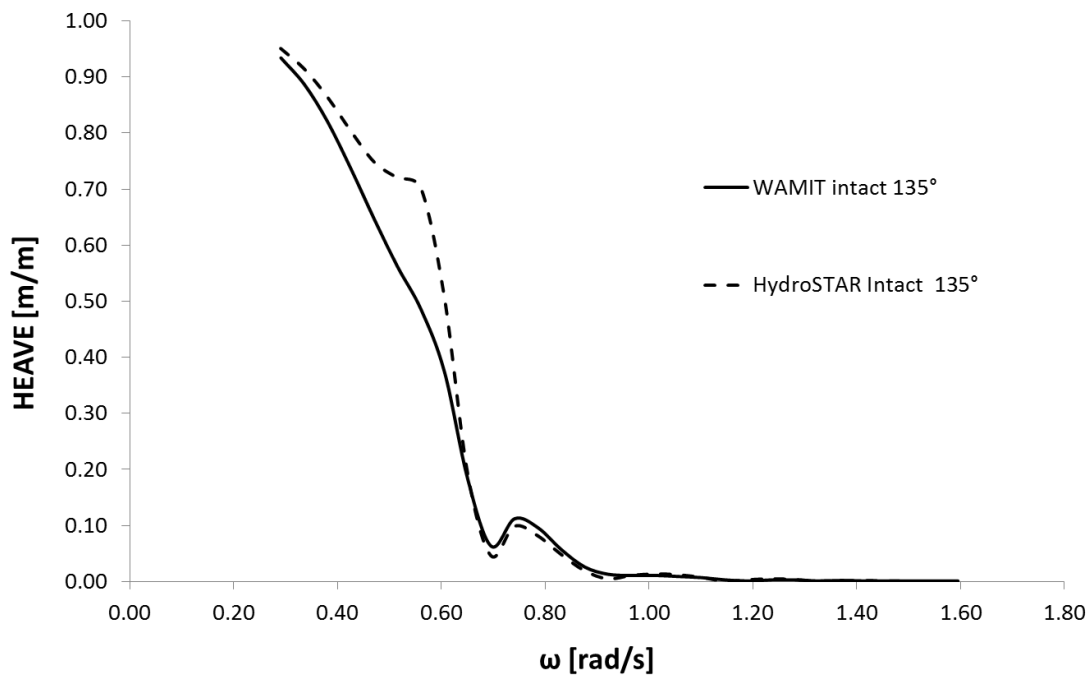
Figure 13 *RAOs of heave motion for bow seas.*

Differences between RAOs of heave motion calculated by WAMIT and the ones obtained from HydroSTAR are noticeable even for intact condition especially in range from 0.4 to 0.6 rad/s. Results for the pitch motion have slightly bigger difference, while also following previously mentioned "rule". Comparative analysis for pitch motion for intact case are given in Figure 14, 15 and 16.
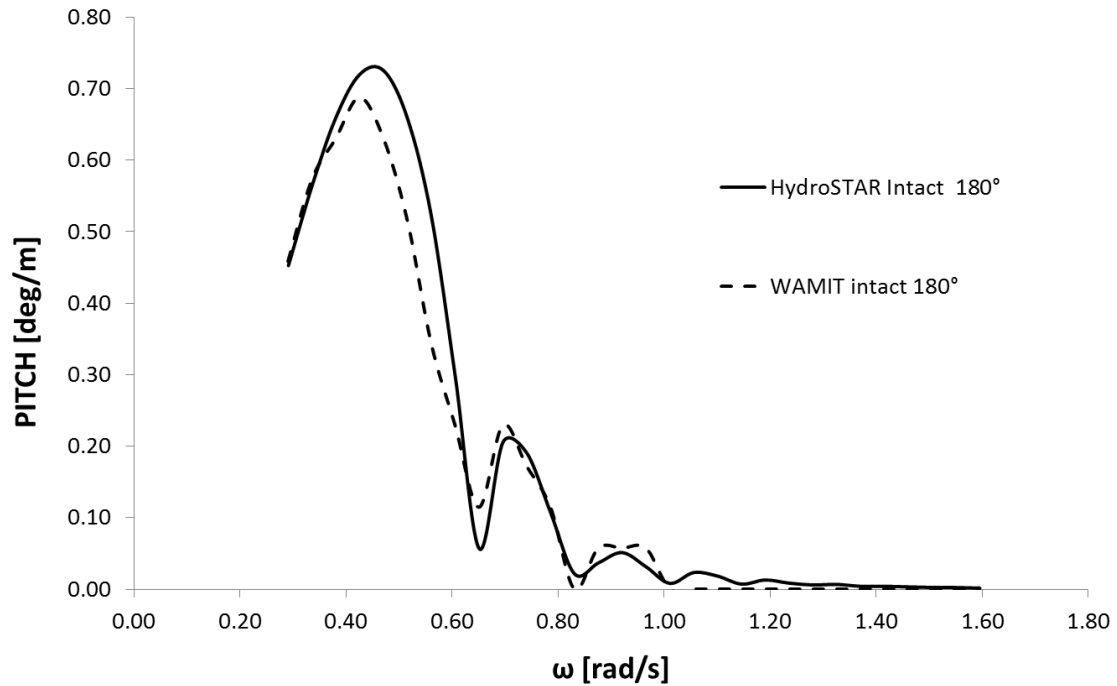
Figure 14 *RAOs of pitch motion for head seas.*
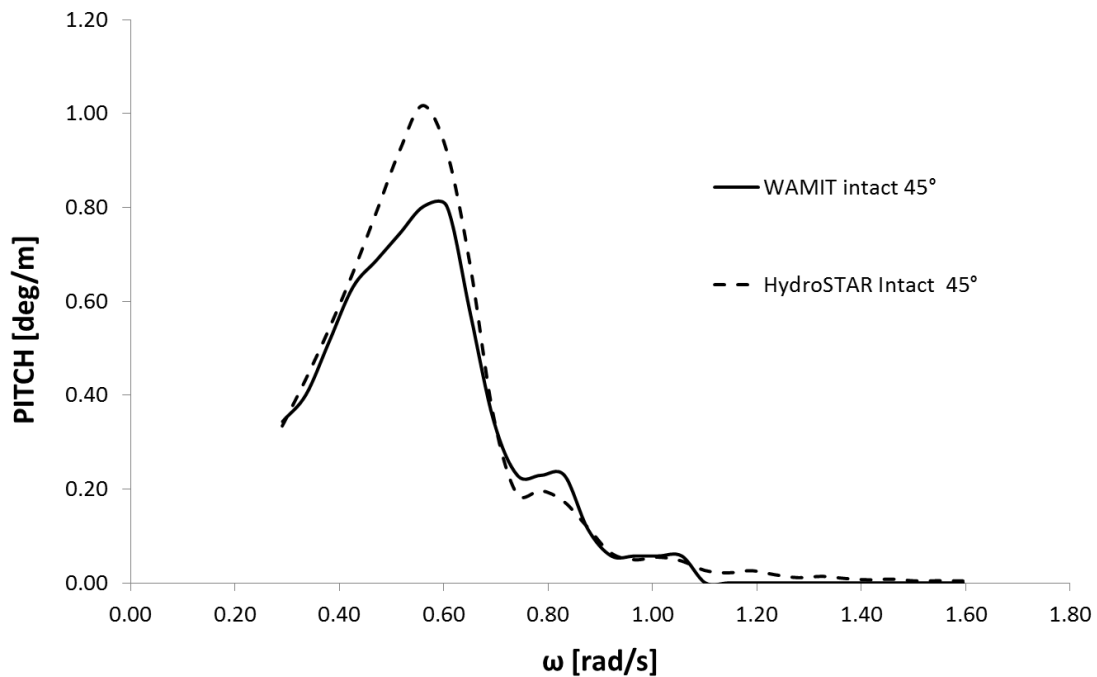
Figure 15 *The RAOs of heave motion for quartering seas.*

It should be noted that mesh used for simulations in WAMIT is different than one For HydroSTAR and since the inclination and trim of the vessel, which is not done in HydroSTAR, results in a lateral and longitudinal displacement of the centre of buoyancy, creating an evident dissymmetry in the restoring forces for heave and especially for pitch motions, some differences had to occur.
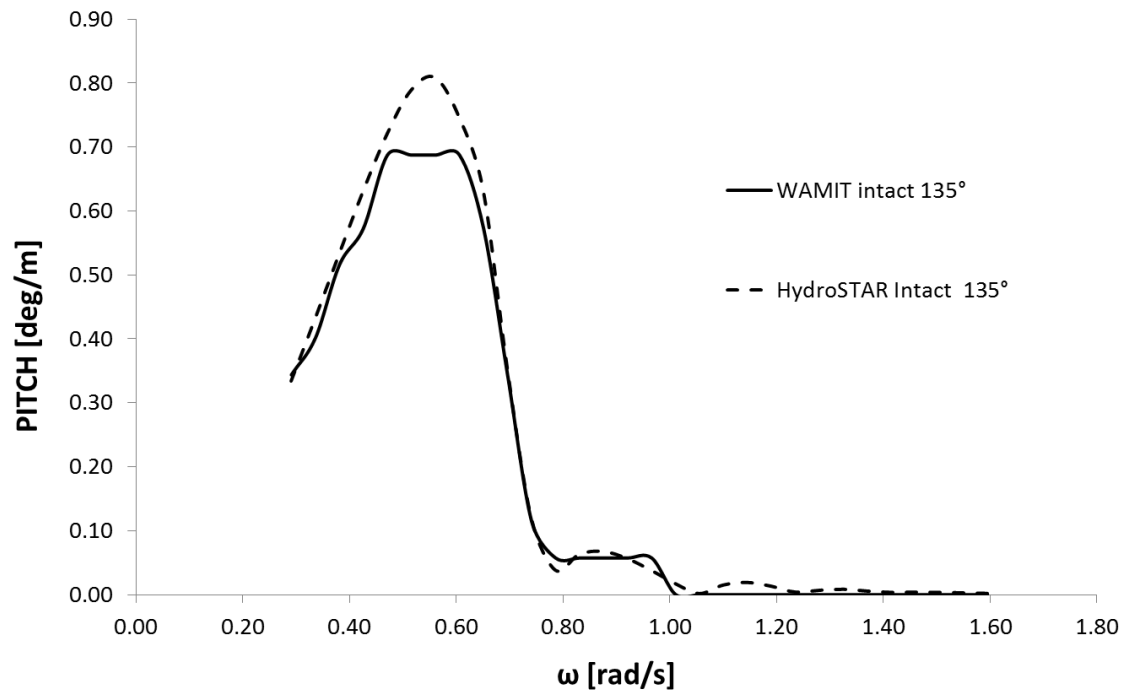
Figure 16 *RAOs of heave motion for bow seas.*

For two grounding damage cases, as well as for intact ship, RAOs of heave and pitch motion for head seas are compared with [21] in Figure 17, 18, 19 and 21.
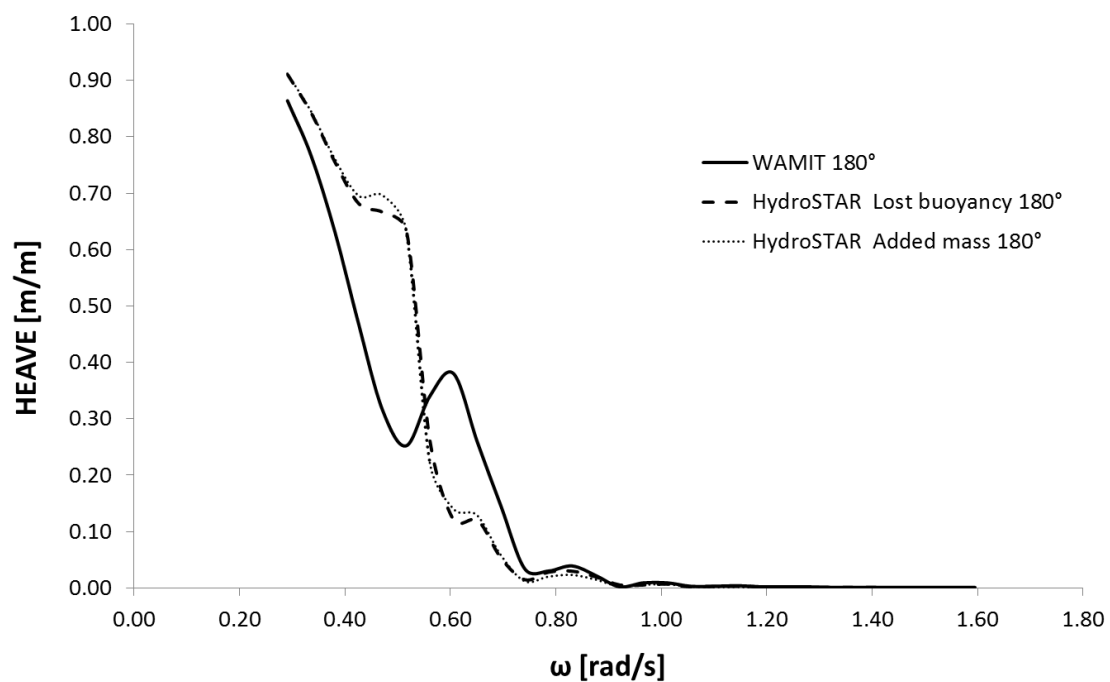
Figure 17 *RAOs of heave motion for head seas DC7.*
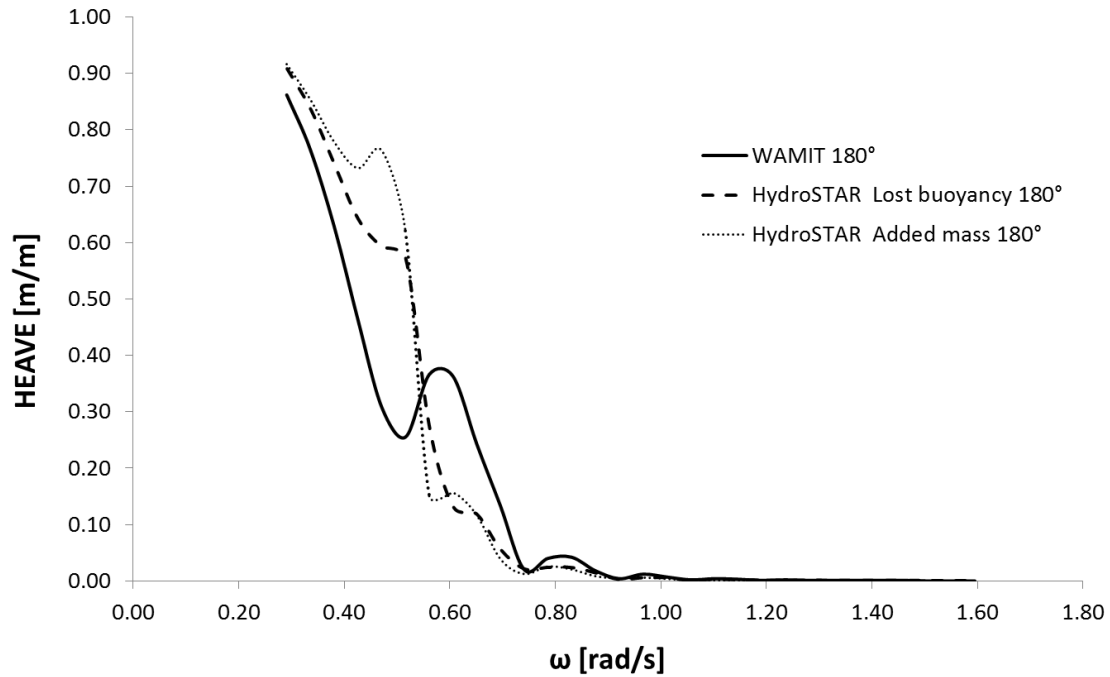
Figure 18 *RAOs of heave motion for head seas DC8.*

Regarding RAOs of ship motion for damage cases one can notice much bigger difference than it was for intact case. Speed of advance along with motion of fluid in internal tanks instead of rigid cargo or lost buoyancy modeling approach is probably the cause of bigger differences.
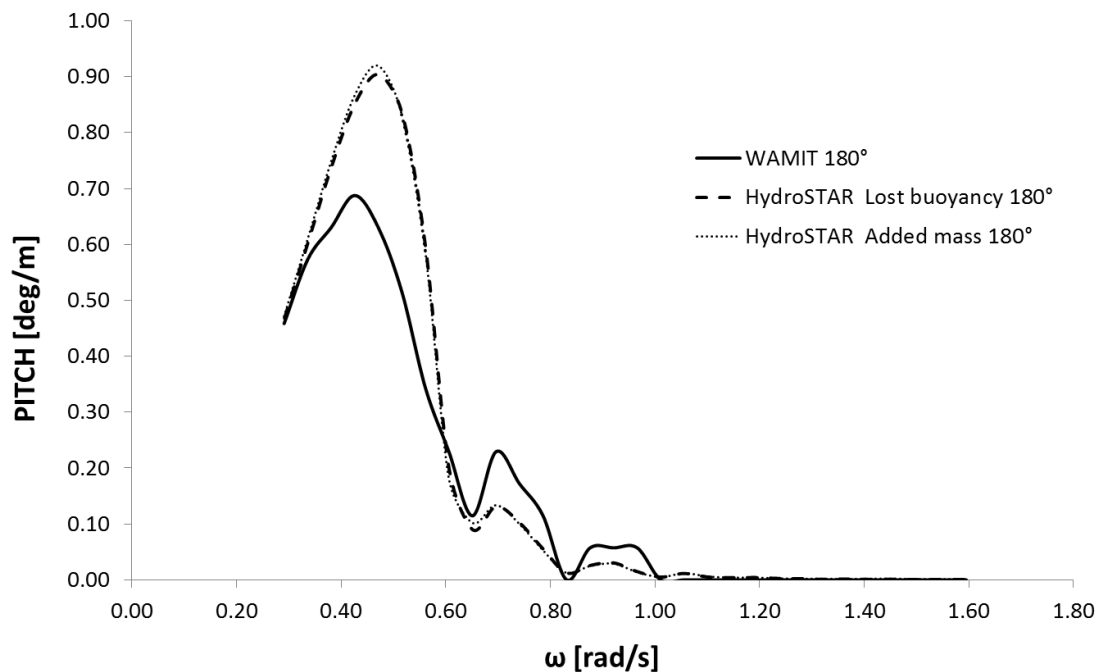
Figure 19 *RAOs of pitch motion for head seas DC8.*
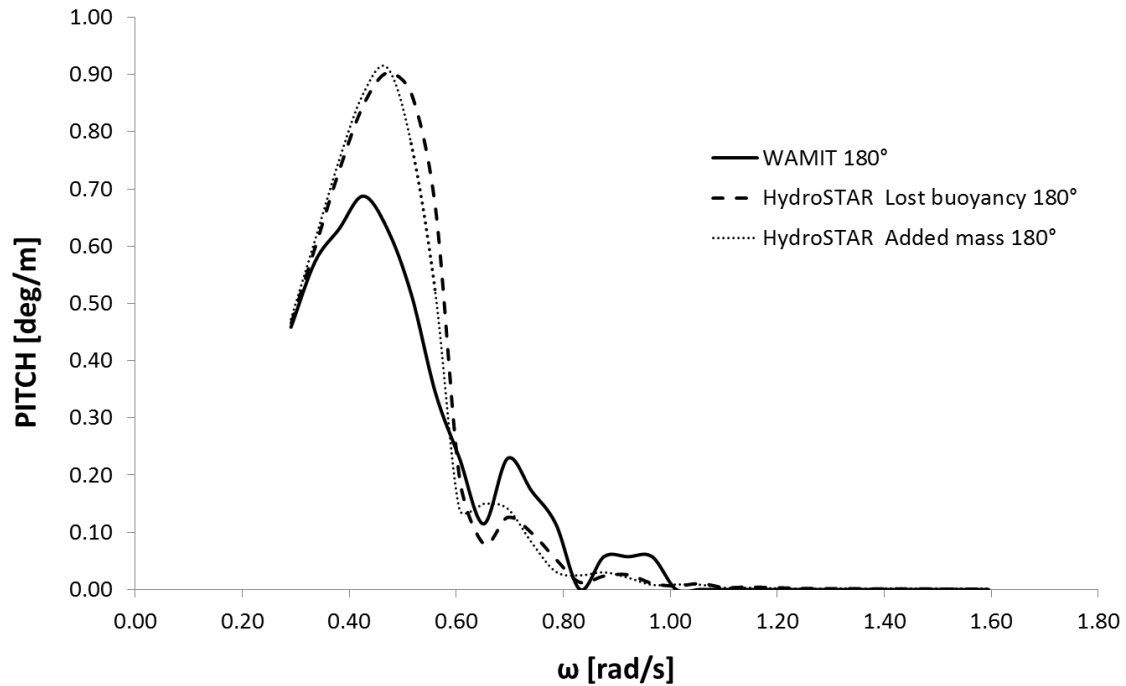
Figure 20 *RAOs of pitch motion for head seas DC8.*

4.2. Comparison between VWBMs calculated by WAMIT and HydroSTAR

RAOs of VWBM amidships are calculated for intact (Figure 21) and for damaged ship. RAOs of VWBM for damaged vessel are determined for two grounding damage cases (Figure 22 and Figure 23). As for the ship motions, constant ship speed of 5 knots is assumed for cases run in HydroSTAR, while in WAMIT, speed of advance is set to 0.
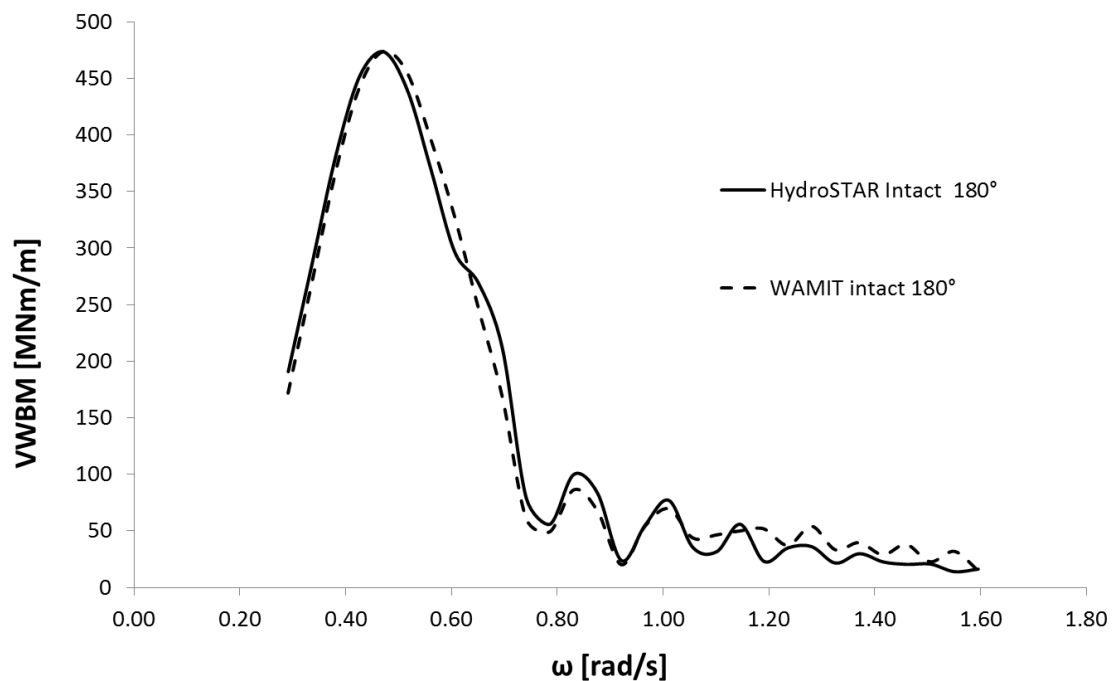
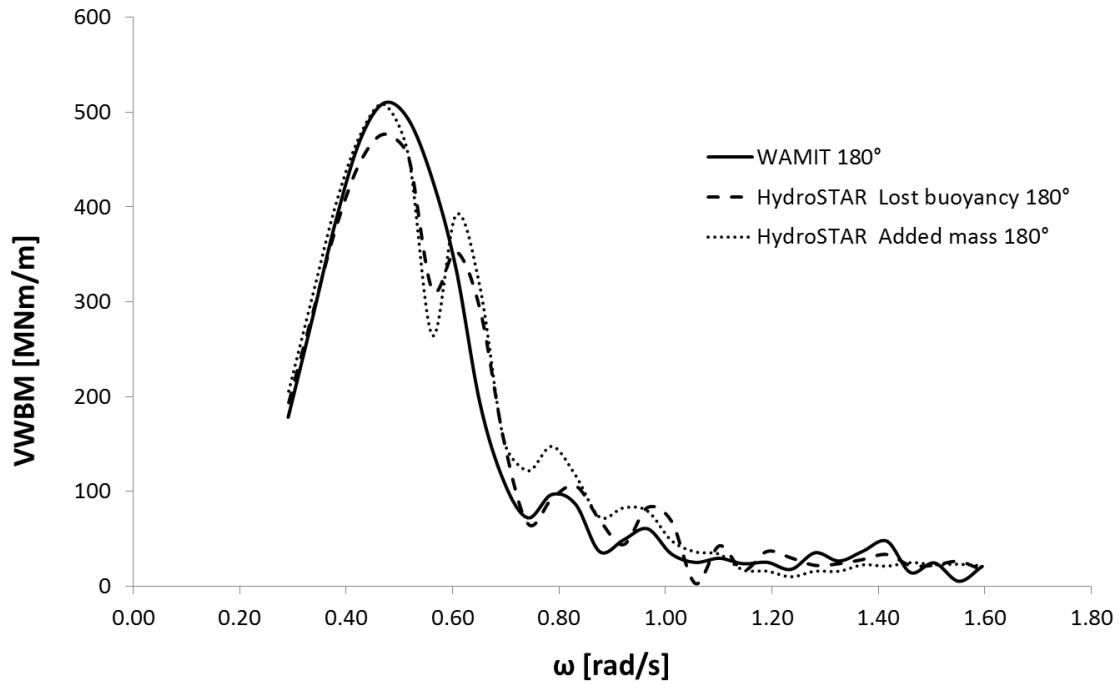**Figure 21** *RAOs of VWBM for head seas, intact condition.*

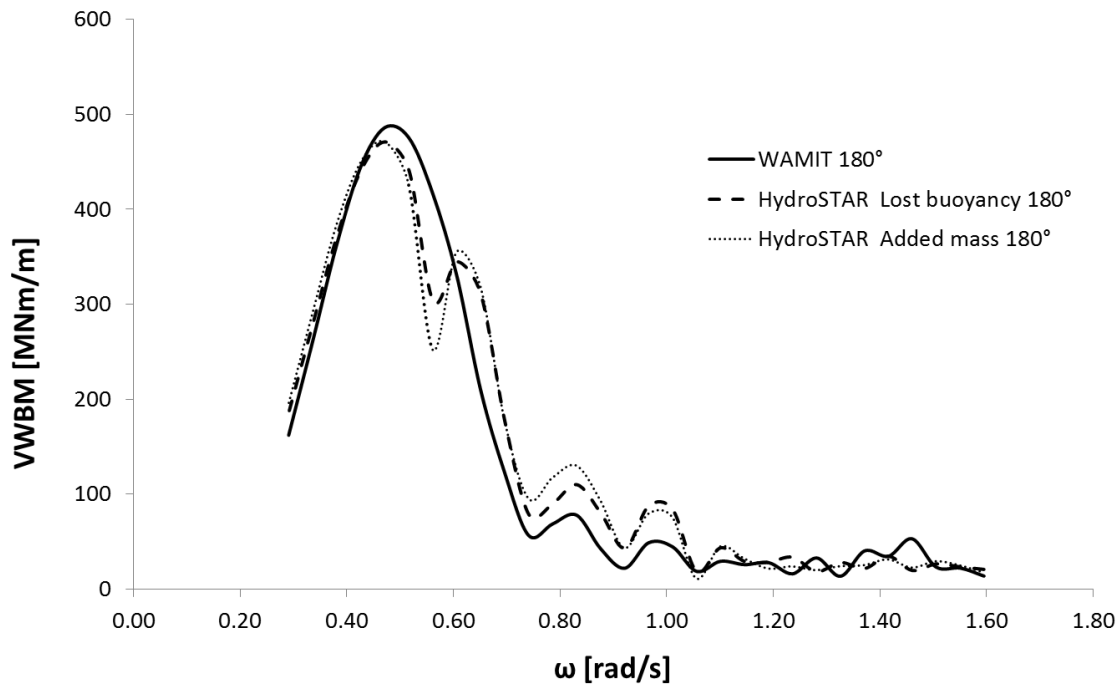**Figure 22** *RAOs of VWBM for head seas DC8.*

Figure 23 *RAOs of VWBM for head seas DC7.*

Looking at the previous 3 figures one can conclude that RAOs of ship VWBM are acting like RAOs of ship motion. Hence for damage cases one can notice much bigger difference than it was for intact case. Speed of advance set to 0 instead of 5 knots along with motion of fluid in internal tanks instead of rigid cargo or lost buoyancy, is probably the cause of bigger differences.

4.3. Distribution of vertical wave loads

Distribution of vertical wave loads for wave frequency where vertical wave loads reach maximum is presented in Figure 24 and Figure 25. Theoretically, vertical loads should reach zero value at the end, but due to inaccurate numerical integration method that force balance has not obtained in any case. For higher frequencies force unbalance at the end becomes bigger but for majority of cases it is inside 10% range.
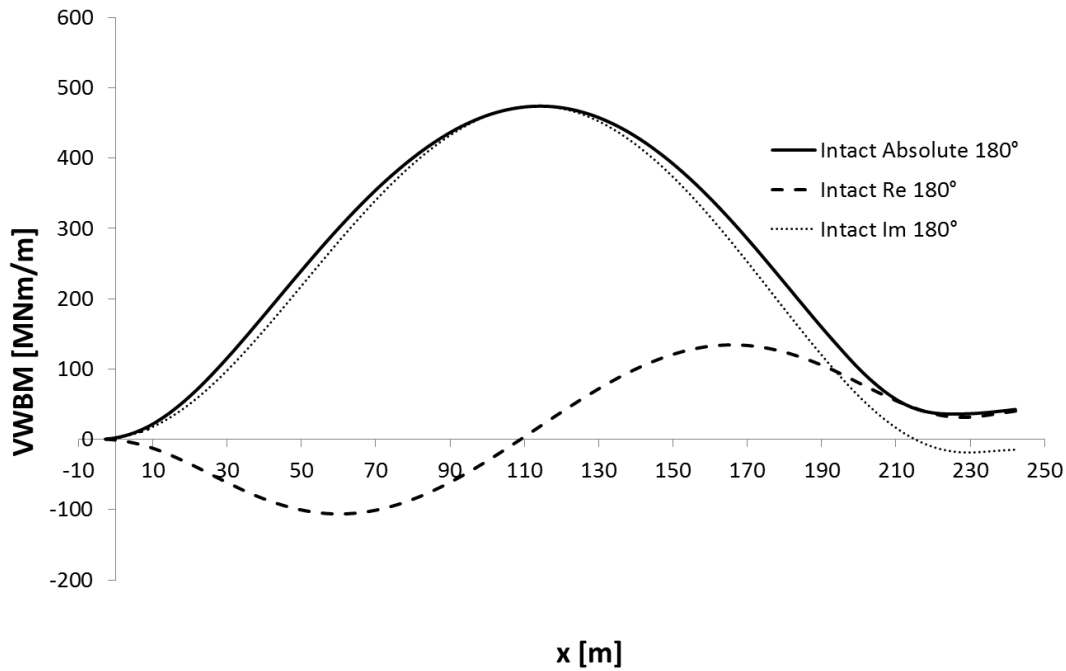

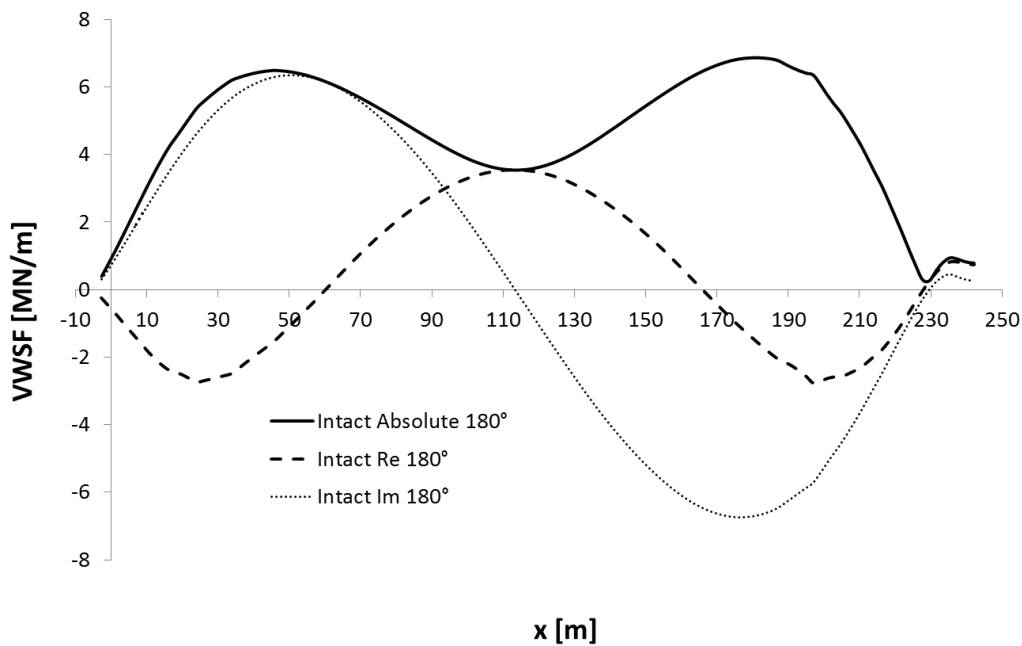**Figure 24** *Distribution of VWBM for intact condition (ω=0.4712 rad/s).*

Figure 25 *Distribution of VWSF for intact condition (ω=0.4712 rad/s).*

4.4. Comparison of ship vertical wave loads for intact and damage condition

RAOs of VWBM amidships are calculated and compared both for intact and for damaged ship case. Most of collision damage cases presented in Figure 26 and both grounding damage case presented in Figure 28 are taken into a consideration. Also RAOs of VWBM at amidships for different wave headings in intact condition are presented in Figure 27.
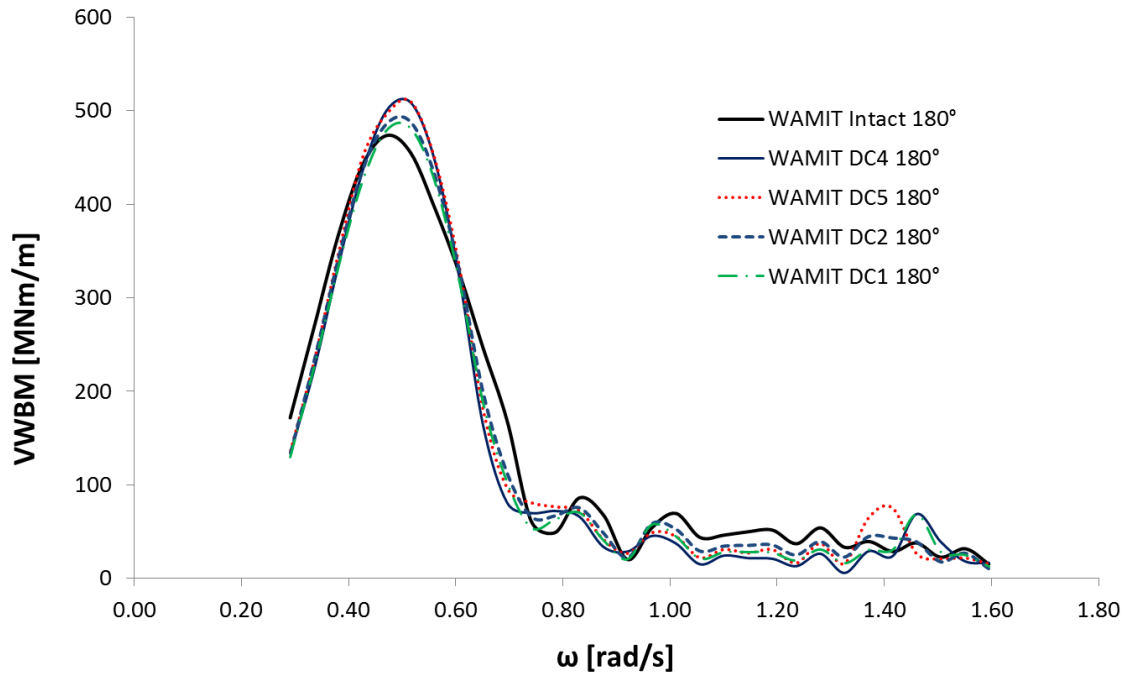

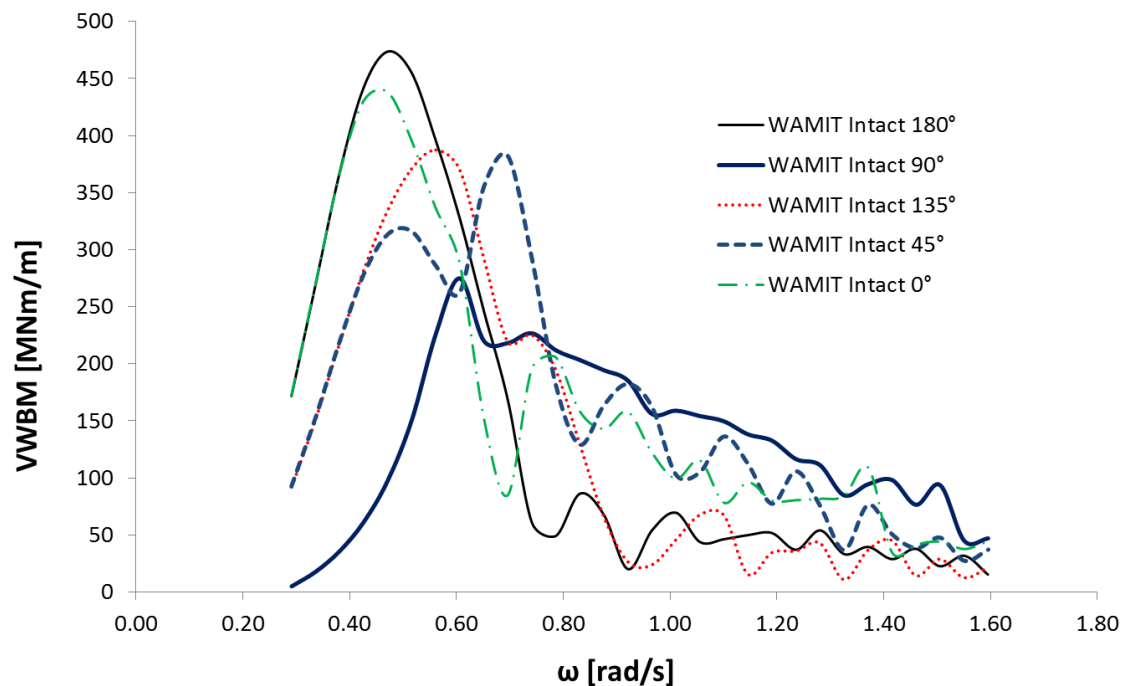**Figure 26** *RAOs of VWBM for head seas, collision DCs.*

Figure 27 *RAOs of VWBM for different wave headings of intact condition.*
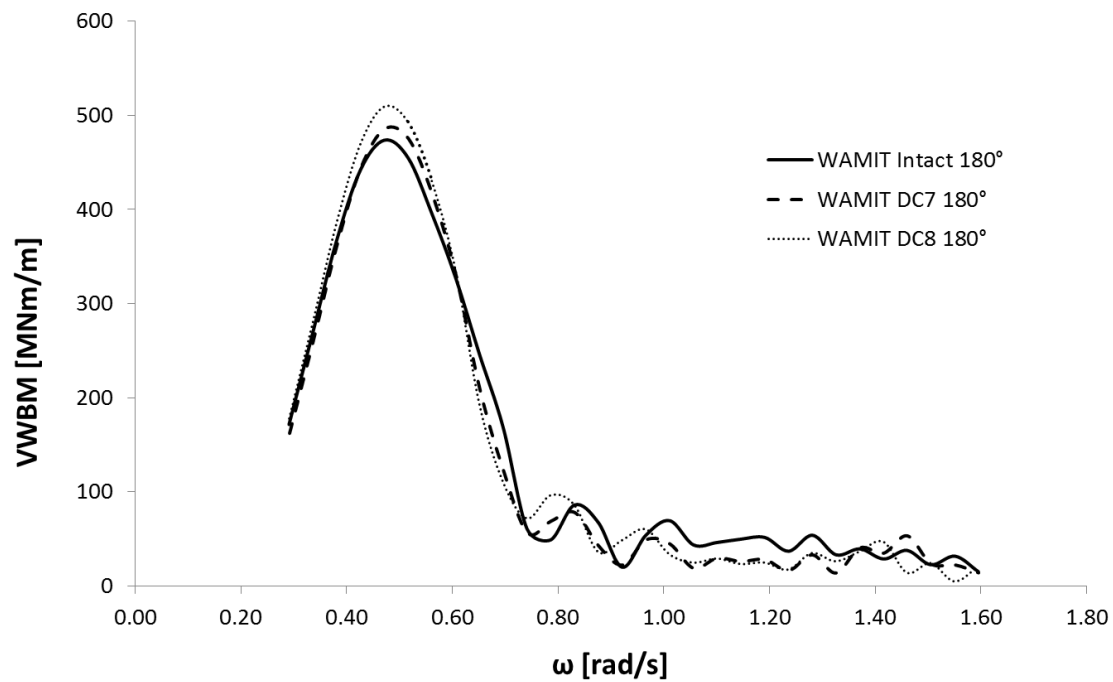
Figure 28 *RAOs of VWBM for head seas, grounding DCs.*

From looking at Figure 26 and Figure 28 one can conclude there are some differences in maximum values of VWBMs between intact and damage condition for head seas. It is also noticeable that maximum values for damage condition occurs at almost same angular frequencies as intact condition.

4.5. Comparison of maximum VWBM at amidships for different heading angles

Maximum VWBM for different wave heading angles are presented in Figure 29. One can see that bow quartering and head seas are toughest cases. Biggest increase of VWBM with respect to intact condition occurs for DC 5 and 8 at heading angle β=225° and is almost 25%.
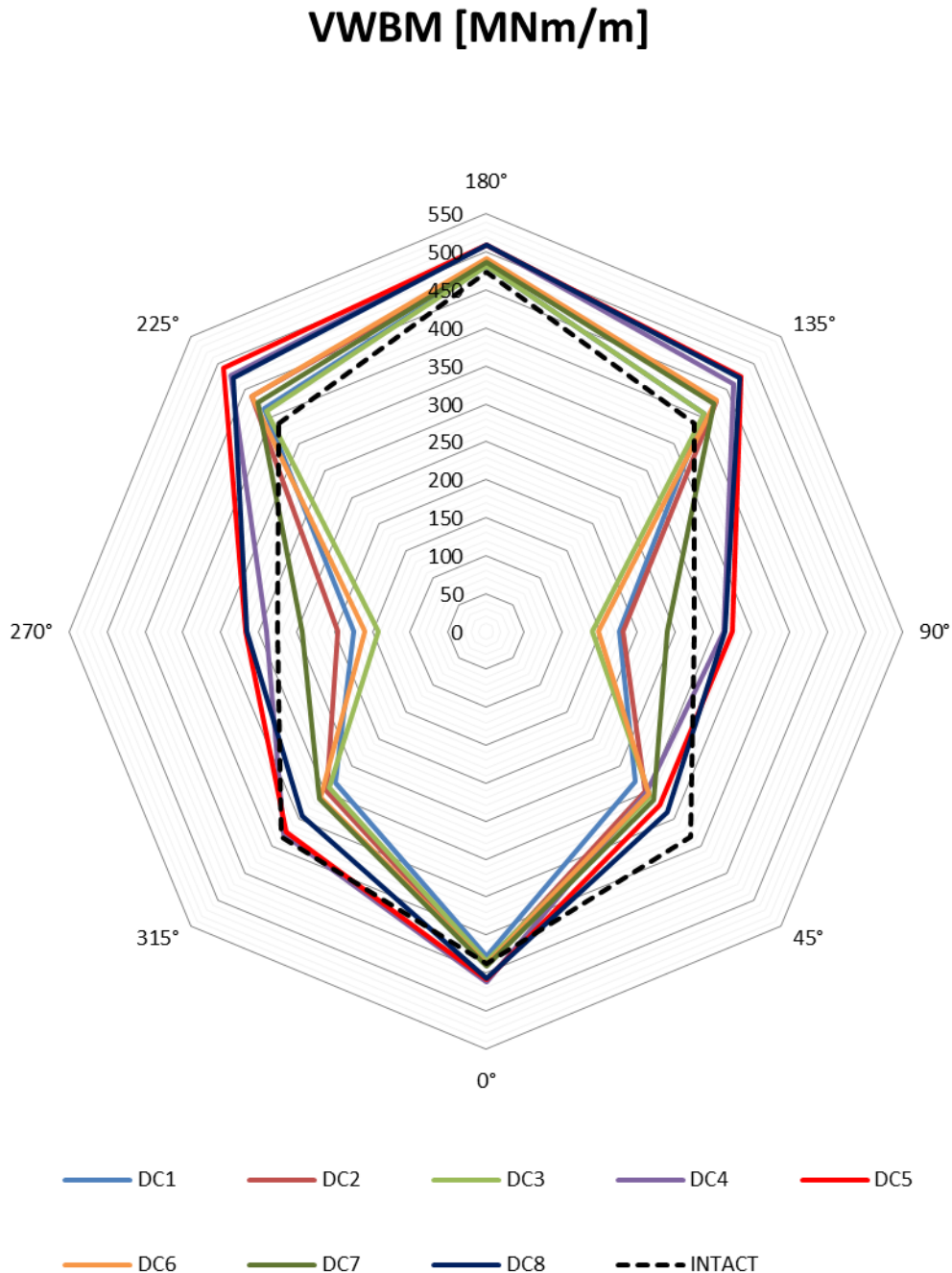

Figure 29 *Maximum VWBM for different wave heading angles.*

One should notice that for most of DCs following and beam sea denotes decrease of VWBM with respect to intact condition e.g. for DC1, with β=225° VWBM is about 25% lower. Even

greater decrease of VWBM regarding to intact condition occurs for some other cases at beam seas. Maximum VWSF for different wave heading angles is presented in Figure 30 and presented diagram it is almost opposite to VWBM diagram. Head seas are lowering SF while following increases it. DC5 and 4 have the biggest value.
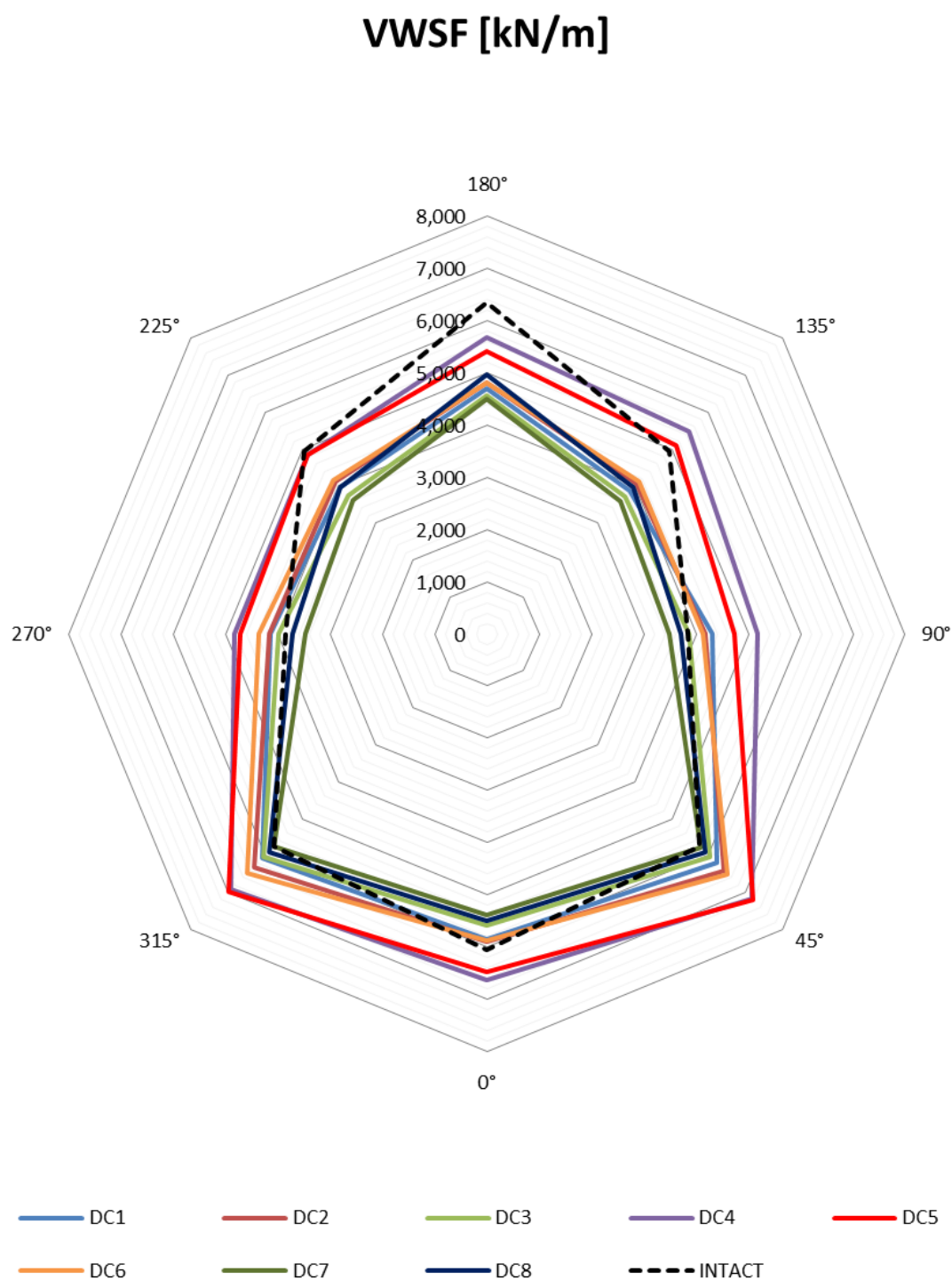

Figure 30 *Maximum VWSF for different wave heading angles.*

In Figure 31, maximum heave motion is presented. There are no big increases or decreases, intact condition has the lowest values, while maximum for heave motion is during beam seas.
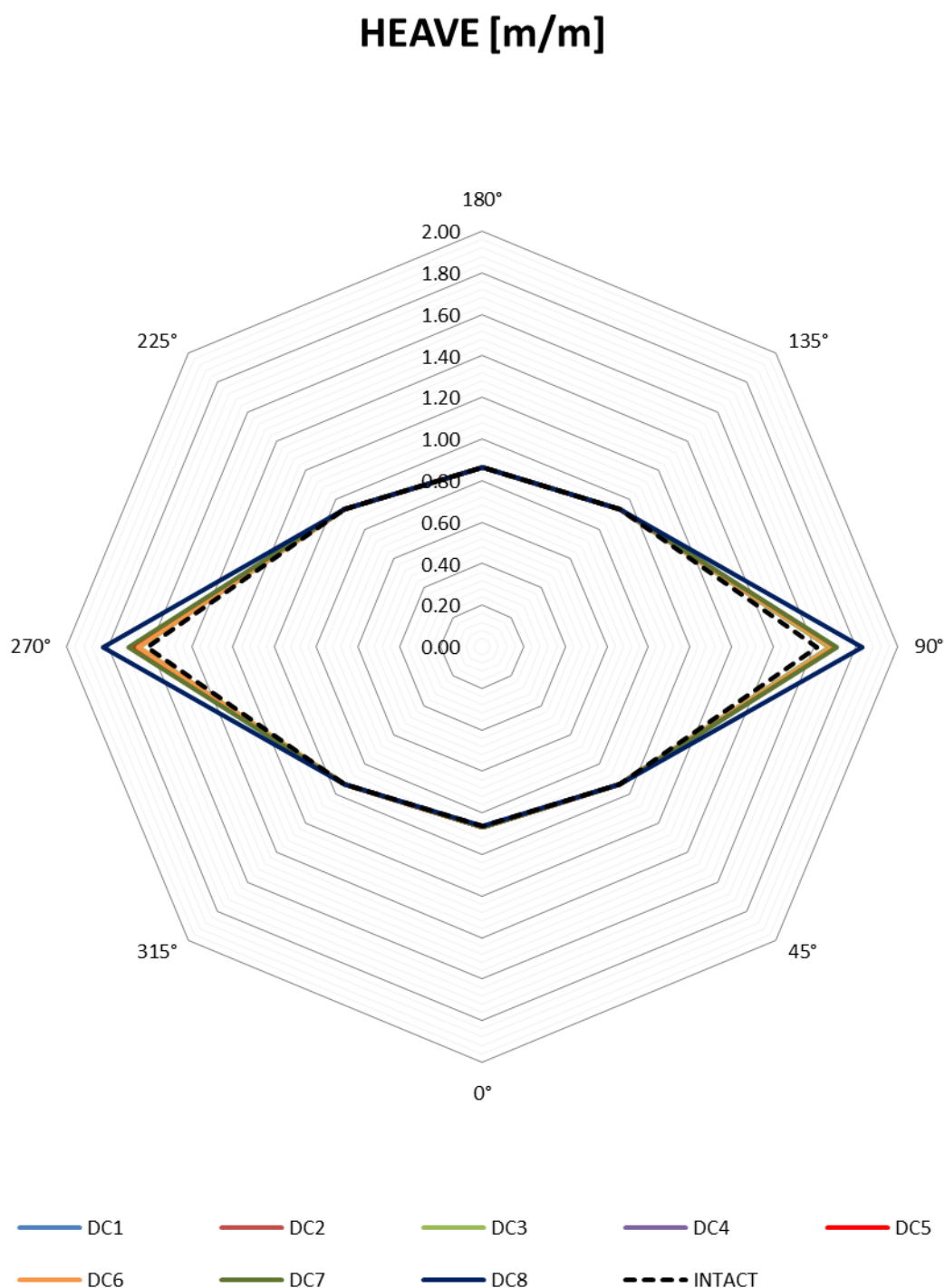
HEAVE [m/m]

Figure 31 *Maximum heave motion for different wave heading angles.*

Maximum pitch motion is presented in Figure 32. Same as for heave, no big increases or decreases of maximum amplitude of motion are noticed for quartering seas.
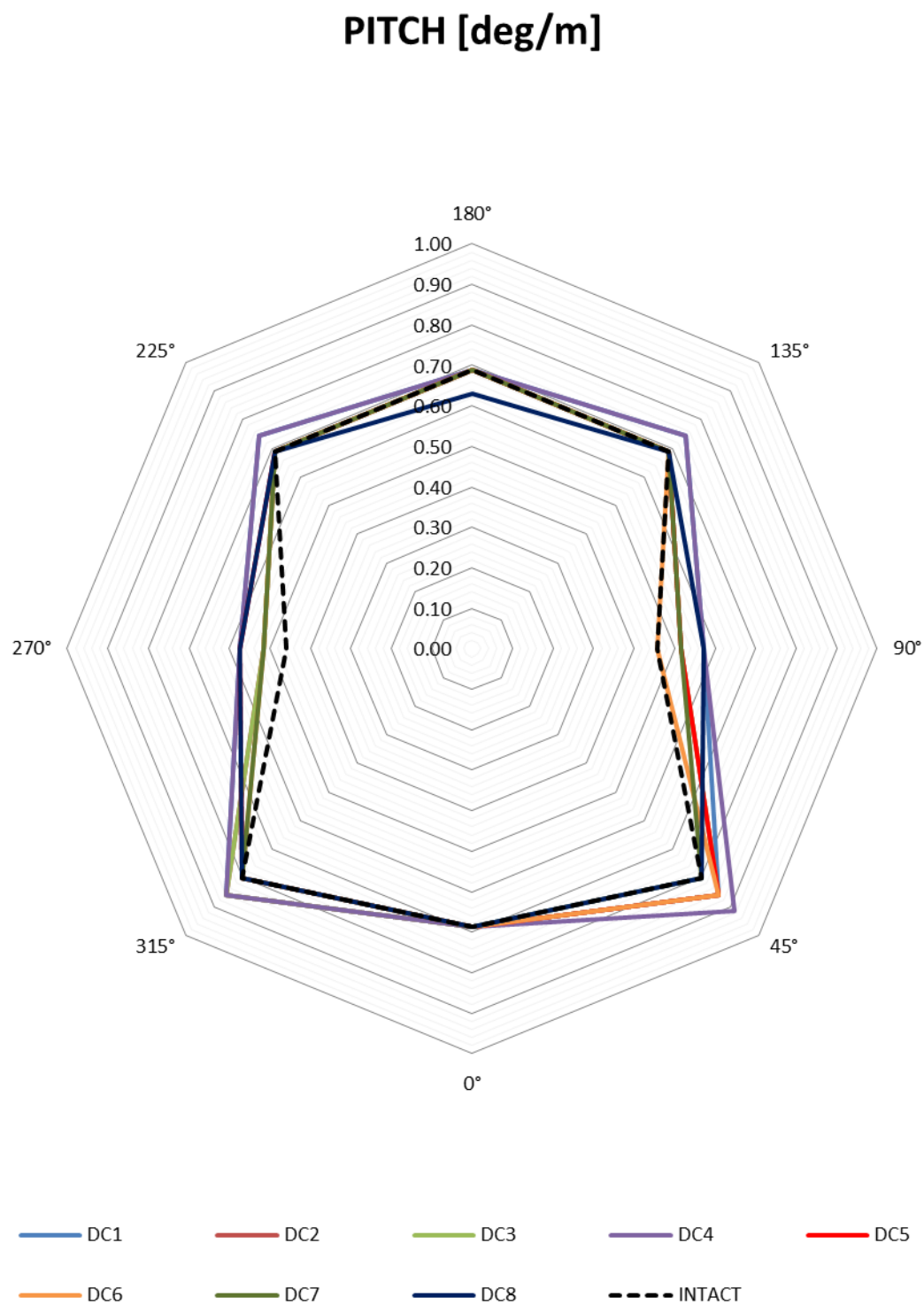
PITCH [deg/m]

Figure 32 *Maximum pitch motion for different wave heading angles.*

5. DISCUSSON

MATLAB code, as can be seen from Figure 27 and Figure 28, is not fully force balanced, and probably some of the reasons are inaccuracy of numerical integration method as well as constant pressure distribution assumption along the panel surface. Also, there are some inconsistencies in input data that occurred due to missing ship data. Unfortunately, due to insufficient time and computer resources those problems have not been resolved completely. Regardless of the previously reported computer code shortcomings, results around global extremes are good, hence maximum VWBM or SF, like in Figure 29, and can be used for further research. Even without computation of global vertical loads developed code still offers a quick and relatively easy way to generate and simulate a lot of different cases.

Maximum VWBM for some damage cases is significantly increased regarding to intact condition at bow quartering seas while at stern quartering and beam seas is significantly decreased. Surprising fact is that while VWBM is decreased for some wave headings, ship motions are always decreasing. Therefore, it can be useful for future research work e.g. to study optimal heading angle for any loading or damage case. Furthermore it is possible to study effect of loading ballast in order to lower the motion and loads by changing mass distribution and also by superimposing force induced by motion of fluid inside the tank.

Linear method is used in this thesis, tanks are already almost full and hull is left undamaged, so it would be interesting to study motion and loads with different amount of fluid inside of the tank before ship reaches quasi-static equilibrium.

Horizontal wave bending moment as well as torsional moments are not included in the present analysis but definitely need further investigation. With not so many adjustments presented code will be able to calculate horizontal wave bending moment along with torsional moments. That should be a next step after debugging is finished.

Aspect that has not been included, yet disserving attention is the influence of the sloshing of liquid in damaged compartments. There is a lot of uncertainty and lack of research in this field.

Finally, the effect of structure opening on hydrodynamic interaction with the waves is also neglected and deserves further research.

6. CONCLUSION

The thesis presented a code for automated hydrodynamic simulations and computation of vertical wave induced global loads. Wave-induced global loads and motions of a ship in intact and damaged conditions are investigated. Flooding scenarios investigated are represented by water ingress into the ballast tanks while the hull is left undamaged. For each investigated case, response amplitude operators of ship motions are calculated using WAMIT, linear 3D panel hydrodynamic code in the frequency domain. The wave-induced global loads are computed using presented code for post processing developed in MATLAB. Even though presented code has not achieved perfect balance in terms of forces, it could be used reliably in wave frequency range from 0.3 to 1.2 rad/s.

Maximum VWBM for some damage cases is significantly increased regarding to intact condition at bow quartering seas while at stern quartering and beam seas is significantly decreased. Surprising fact is that while VWBM is decreased for some wave headings ship motions are always decreasing. Therefore, for future research work would be interesting to study optimal heading angle or effect of loading ballast in order to lower the motion and loads.

The obtained results are also compared with ones computed in HydroSTAR, published by [21]. Comparing results for RAOs of ship motion for intact condition some differences can be noticed. Those differences are getting even bigger for damage cases. Some differences are noticed for results of VWBMs since wave moments depend on ship motion in waves. Usage of different mesh while also including inclination and trim of the vessel along with motion of fluid in internal tanks and included speed of advance are probably the reasons for differences, but further research is necessary for obtaining more reliable conclusions.

BIBLIOGRAPHY

[1] Chan, H. S., Atlar, M. and Incecik, A. (2003). "Global wave loads on intact and damaged RO-RO ships in regular oblique waves", *J Marine Structures* Vol. 16, pp.323-344.

[2] Chan, H.S., Incecik, A. and Atlar, M. (2001). "Structural Integrity of a Damaged Ro-Ro Vessel" *Proceedings of the second international conference on collision and grounding of ships*, Technical University of Denmark, Lyngby, pp. 253-258.

[3] Downes, J., Moore, C., Incecik, A., Stumpf, E., and McGregor J. 2007. A Method for the quantitative Assessment of Performance of Alternative Designs in the Accidental Condition, *10th International Sympo- sium on Practical Design of Ships and Other Floating Structures*, Houston, Texas.

[4] DNV (2010): Global performance analysis of deep water floating structures, Recommended practice, DNVRP-F205

[5] Edward V. Lewis, Principles of Naval Architecture Second Revision, Volume I, SNAME New Jersey 1988

[6] Folsø, L., Rizzuto E., and Pino E. 2008. Wave Induced Global Loads for a Damaged Vessel, *Ships and Offshore Structures*, Volume 3, No.4, pages 269-287.

[7] H. Jafaryeganeh, J.M. Rodrigues & C. Guedes Soares, 2014. Influence of mesh refinement on the motions predicted by a panel code *Maritime Technology and Engineering – Guedes Soares & Santos (Eds)* Taylor & Francis Group, London, ISBN 978-1-138-02727-5.

[8] Hirdaris, S., Argiryiadis, K., Bai, W., Dessi, D., Ergin, A., Fonseca, N., Gu, X., Hermundstad, O. A., Huijsmans, R., Iijima, K., Nielsen, U.D., Papanikolau, A., Parunov, J. and Incecik, A. 2014. Loads for use in the design of ships and offshore structures, *Ocean engineering*, 78, pp. 131–174.

[9] IACS, 2012. *Harmonized Common Structural Rules, External release*, 1st July 2012.

[10] IMO Revised, 2003. Interim guidelines for the approval of alternative methods of design and construction of oil tankers under Regulation 13F(5) of Annex 1 of MARPOL 73/78, *Resolution MEPC 2003*;110(49), Annex 16.

[11] J. M. J. Journée and W. W. Massie, Offshore Hydromechanics, First edition, Delft University of Technology, 2001.

[12] Ko, H-K., Park, T., Kim, K-H., Kim, Y., Yoon, D-H (2011): Development of panel generation system for seakeeping analysis, *Journal of Computer-Aided Design*, Vol. 43, pp. 848–862.

[13] Korkut, E., Atlar, M. & Incecik, A. 2004. An experimental study of motion behavior with an intact and dam- aged Ro-Ro ship model, *Ocean Engineering*, Vol. 31, pp. 483–512.

[14] Korkut, E., Atlar, M. and Incecik, A. (2005), "An experimental study of global loads acting on an intact and damaged Ro–Ro ship model", *J Ocean Engineering* v.32, pp.1370-1403.

[15] Lee, Y., Chan, H.-S., Pu, Y., Incecik, A., and Dow, R. S., 2012. Global wave loads on a damaged ship, *Ships and Offshore Structures*, 7(3). pp. 237–268.

[16] Lloyd's Register, (2000). *"World Casualty Statistics: annual statistical summary of reported loses and disposals of propelled sea-going merchant ships of not less than 100 GT".*

[17] Luis, R.M., Teixeira, A.P., and Guedes Soares, C., 2009. Longitudinal strength reliability of a tanker hull accidentally grounded, *Structural Safety*, Volume 31, Issue 3, pp. 224–233.

[18] Mohammadi, M., Khedmati, M. R., and Vakilabadi, K. A., 2014. Effects of hull damage on global loads acting on a trimaran ship, Ships and Offshore Structures, Vol. 10, Iss. 6, 2015

[19] Faltisen O. M., Sea Loads on Ohips and Offshore Structures, Cambridge Ocean Technology Series, Cambridge, 1990.

[20] Parunov, J, Ćorak, M and Gledić, I. 2015. Comparison of two practical methods for seakeeping assessment of damaged ships, Analysis and Design of Marine Structures, Guedes Soares & Shenoi (Eds), Taylor and Francis Group., pp. 37–44.

[21] Parunov, J, Ćorak, M, I. 2015. Design charts for quick estimation of wave loads on damaged oil tanker in the Adriatic Sea, Towards Green Marine Technology and Transport – Guedes Soares, Dejhalla & Pavleti (Eds), Taylor & Francis Group, London, UK, pp. 389–395.

[22] Prestileo, A., Rizzuto, E., Teixeira, A.P., and Guedes Soares, C., 2013. Bottom damage scenarios or the hull girder structural assessment, *Marine Structures*; 33, pp. 33–55.

[23] Teixeira, A.P., and Guedes Soares, C. 2010. Reliability assessment of intact and damaged ship structures. In: Guedes Soares, C., Parunov, J. (Eds.), *Advanced Ship Design for Pollution Prevention*. Taylor and Francis Group, London, ISBN: 978-0-41558477-7.

[24] WAMIT User manual Version 6.4, Massachusetts Institute of Technology, Boston 2006.

[25] Čorić, V.; Prpić-Oršić J.: *Pomorstvenost plovnih objekata*; Zigo, Rijeka, 2006

[26] http://geomalgorithms.com/a01-_area.html